Institute for Problems in Mechanics of the Russian Academy of Sciences

Laboratory of Applied Continuum Mechanics

Final Report

on Research Contract

“ Alternative Approach to Compositional Simulations (AltSim-2)”

Acting Director of the Institute for Problems in Mechanics RAS	Corresponding Member of RAS, Professor N.A.Generalov
Principal Investigator	Professor V.M.Entov, Dr. Sci
Investigators	Senior Research Associate Dr.A.V.Myasnikov Senior Engineer Kh.Kh.Ilyasov Research Associate A.K.Kozlova Ph.D.Student K.O.Samoylov

Moscow, June 28, 2004

Contents

1 Introduction

This Report describes results of studies during the period of July,03-June,04 on development of an ECLIPSE-compatible version of compositional simulator based on alternative description of phase equilibria in multicomponent systems. It is a direct continuation of the Project “AltSim” (2001-2002) (see Reports [1], [2], [3]). The main idea of the alternative approach is to make use of specific geometry of two-phase domain of the compositional space of multicomponent systems, namely the fact that all compositions along a straight tie-line in compositional space break into gaseous and liquid phases of the same compositions, and only relative amounts of the phases vary along each tie-line. Therefore, a vector-parameter of tie-lines $\boldsymbol{\gamma}$ and a scalar ‘leading component concentration’ C appear to be natural variables for description of composition and phase equilibria. Hence the description of phase equilibria in terms of these variables looks promising both in the sense of better understanding underlying physics and computationally. This basic idea has been conceptually confirmed by previous research described in Reports [1], [2], [3], (see also [4] – [13]).

Present study is concentrated primarily on computational aspects of the approach. Its main objective is to develop an “alternative compositional block” which could be incorporated into existing ECLIPSE simulator with minimum modifications of the existing structure in the hope that possible advantages of the alternative approach combined with well-established efficiency of the main body of the ECLIPSE package may lead to improved performance of compositional simulator. This ‘limited modifications’ approach emerged after several discussions at Abingdon and Moscow, and is adopted as the main strategy of further research. While somewhat limiting potential improvements, it allows to switch to the new procedures without significant modification of the entire simulator structure.

In this respect, this study differs significantly from the previous work in which the main objective was to prove viability of the alternative approach and to develop the respective package architecture.

2 Formulation of the Problem in the N_c Component Case

2.1 Governing Equations

Let us consider a multicomponent system of N_c components that may form a single- phase or two-phase mixture. The mixture state is considered to be completely specified by the pressure P, temperature T and by the composition vector $\mathbf{C} = [C_{1,}C_2, C_3, ..., C_{N_c}]$, where C_k is the molar concentration of the k-th component, which is by definition is the ratio of the number of moles of the i-th component in the mixture to the overall number of moles per unit volume $C_k = b_k/b$, where b and b_k denote respectively overall and partial molar densities.

The system of governing equations can be written in the standard way in the form of component conservation laws:

$$\frac{\partial mb}{\partial t} + div\left(\mathbf{U}^l b^l + \mathbf{U}^g b^g\right) + Q = 0$$

$$\frac{\partial mbC_k}{\partial t} + div\left(\mathbf{U}^l b^l C_k^l + \mathbf{U}^g b^g C_k^g\right) + q_k = 0, \quad k = 1, ..., N_c - 1 \tag{1}$$

where m is the reservoir porosity, C_k^p is the molar concentration of the k-th component for the phase $p = l, g$, b^p is the molar density of the phase p, q_k is the inlux/outflux rate density (contribution of wells) for the k-th component, specified below, and $Q = \Sigma q_k$.

Phase velocities $\mathbf{U}^p$ are found from the Darcy law

$$\mathbf{U}^l = -K(x,y)\frac{k^l(S)}{\mu^l\left(\mathbf{C}\right)} gradP, \quad \mathbf{U}^g = -K(x,y)\frac{k^g(S)}{\mu^g\left(\mathbf{C}\right)} gradP \tag{2}$$

where K is the absolute permeability, k^p is relative permeability of the phase p, μ^p is the viscosity of the phase p. Within the two-phase domain, the overall molar density is found from the expression

$$b = b^l S + b^g(1-S), \quad S = \frac{L}{L + (b^l/b^g)(1-L)}, \quad L = \frac{C_1 - C_1^g}{C_1^l - C_1^g}. \tag{3}$$

where L is the molar fraction of the liquid phase, S is the saturation, or volume fraction of the liquid phase. To make the system complete, one has to specify the values of b^l, b^g,C_k^l,C_k^g and μ^l, μ^g as functions of $\mathbf{C}$ and P. Let us suppose at the moment that these functions are known:

$$b^p = b^p\left(\mathbf{C}, P\right), \quad C_k^p = C_k^p\left(\mathbf{C}, P\right), \quad \mu^p = \mu^p\left(\mathbf{C}, P\right). \tag{4}$$

Then the system (1)– (4) can be solved by making use of well-known numerical schemes.

An in-house solver has been developed to be able to check independently effects of separate blocks of the code package. Before describing the algorithm and results, we discuss treatment of wells (sources and sinks), and normalization used below.

2.2 Inflow and Outflow Conditions

In the present study, the following approximation for the the component molar flow rates in vicinity of injecting and producing wells is adopted:

Let Q_{in} and Q_{out} be the overall inflow and outflow molar rates.

For calculations in the present study we use the formulae:

$$Q_{in} = T_w \delta_f \left(\frac{k^l}{\mu^l} + \frac{k^g}{\mu^g}\right)\left(s^l b^l + s^g b^g\right)\left(P_{in} - P\right) \tag{5}$$

$$Q_{ou} = T_w \delta_f \left(\frac{k^l}{\mu^l} b^l + \frac{k^g}{\mu^g} b^g\right)\left(P_{out} - P\right) \tag{6}$$

where

$$T_w = K \frac{\beta}{\ln \frac{r_0}{r_w} + \sigma}, \tag{7}$$

β is the angle segment connecting the grid cell with the well (for well at the center of grid block $\beta = 2\pi$, for a well on a boundary $\beta = \pi$, and into a corner $\beta = \pi/2$), r_0 is the pressure equivalent radius of the cell, r_w is a well radius, σ is the skin factor.

Corresponding molar outflow rate q_k in the two phase domain is

$$q_k = T_w \delta_f \left(\frac{k^l b^l}{\mu^l} C_k^l + \frac{k^g b^g}{\mu^g} C_k^g \right) (P_{out} - P) \, . \tag{8}$$

However, in the injection (inflow) case we just keep the injection-cell composition equal to the one specified in the well.

2.3 Normalization

Below, we denote L_0, μ_0, k_0, P_0, b_0, $V_0 = k_0 P_0 / L_0 \mu_0$, and $t_0 = L_0 / V_0$ some characteristic values of the length, viscosity, permeability, pressure differential, molar density, fluid velocity and time.

Then after transformation to respective non-dimensional variables the equations will have the same form as before.

The following typical values of the scales are assumed below:

$L_0 = 2000m = 2 \cdot 10^3 m$,

$\mu_0 = 0.03 \cdot 10^{-2} P = 3 \cdot 10^{-5} Pa \cdot s$,

$k_0 = 100 \cdot mD == 10^{-13} m^2$,

$P_0 = 30atm = 3 \cdot 10^6 Pa$,

$b_0 = 6.25 \ kgmol \cdot m^{-3}$;

$V_0 = 5 \cdot 10^{-6} \frac{m}{s}$;

$t_0 = 4 \cdot 10^8 s = 4629.6 days$.

3 Numerical Model

3.1 General Structure of Numerical Algorithm

Let us rewrite the system of governing equations in the form

$$-div\left(K\left[\frac{k^l}{\mu^l}b^l+\frac{k^g}{\mu^g}b^g\right]gradP\right)=-Q(P,\boldsymbol{C})-\Delta b; \tag{9}$$

$$mb\frac{\partial C_k}{\partial t}-div\left(K\left[\frac{k^l}{\mu^l}b^lC_k^l+\frac{k^g}{\mu^g}b^gC_k^g\right]gradP\right)=-q_k(P,\boldsymbol{C})-C_k\Delta b, \tag{10}$$

where $\Delta b=\partial mb/\partial t$. Let us assume that at the moment $t=t^n$ the values of Δb, of the mixture pressure P, composition vector $\boldsymbol{C}$ and functions (3) and (4) are known.

Then to determine the values of the variables at the next time step, $t=t^{n+1}$, we arrange the iterative procedure as follows (below, for the sake of simplicity, we write the discretization of Eqs.(9) and (10) for one-dimensional case only):

$$\frac{P_i^q-P_i^n}{\alpha\tau}-\widetilde{K}_{i+1/2}^r\frac{P_{i+1}^q-P_i^q}{h_x^2}+\widetilde{K}_{i-1/2}^r\frac{P_i^q-P_{i-1}^q}{h_x^2}=\widetilde{Q}_i^r \tag{11}$$

$$(mb)_i^q\frac{C_{k,i}^q-C_{k,i}^n}{\tau}-\widehat{K}_{i+1/2}^r\frac{P_{i+1}^q-P_i^q}{h_x^2}+\widehat{K}_{i-1/2}^r\frac{P_i^q-P_{i-1}^q}{h_x^2}=\widehat{Q}_i^r \tag{12}$$

$$\widetilde{K}=K\left[\frac{k^l}{\mu^l}b^l+\frac{k^g}{\mu^g}b^g\right],\quad \widetilde{Q}=-Q-\Delta b \tag{13}$$

$$\widehat{K}=K\left[\frac{k^l}{\mu^l}b^lC_k^l+\frac{k^g}{\mu^g}b^gC_k^g\right],\quad \widehat{Q}=-q_k-C_k\Delta b. \tag{14}$$

Here, α is an artificial compressibility relaxation parameter.

At the first iteration, we put $r=n$ and from Eq.(11) obtain P^q which then is used in Eq. (12) to obtain C_k^q. The values P^q and $\boldsymbol{C}^q$ are used then to determine functions $(b^p)^q$, $(C_k^p)^q$, $(\mu^p)^q$ in accordance with equations of state Eq.(4). These values, in turn, are used to determine the quantities at the next iteration (with the superscript r), which is set hereafter to

$r = (n+q)/2$. The iterations at each time step are continued until $|(\Delta b^q - \Delta b^{q-1})/\Delta b^{q-1}| \geq \varepsilon$.

The question is how to calculate functions with the semi-integer subscript $i+1/2$, i.e. defined on the intergrid boundaries. We need to know there phase densities, relative permeabilities and phase viscosities which all are functions of composition determined at the center of the cell. In the present study, we use the simplest upwind specification for all the listed functions: $f_{i+1/2} = f_i$ if $P_{i+1} - P_i < 0$, and $f_{i+1/2} = f_{i+1}$ otherwise.

3.2 ECLIPSE's EOS Solver $flashs$

The pivotal point of the described above iterative procedure is the assumed possibility to specify the thermodynamic state of the phases (4) by the given values of the mixture pressure P and the composition vector $\boldsymbol{C}$.

The possibility is realized in the subroutine *flashs* from the ECLIPSE package for compositional simulation of a range of petroleum reservoir engineering problems. The subroutine, which in fact summarizes different approximations of the equation of state tables by several chosen well known cubic polynomials, is considered in the present study as a 'black box' which returns the compositions of the phases C_k^p and their molar densities b^p as output data, the input data being the pressure P and overall composition $\boldsymbol{C}$.

Coupled with another ECLIPSE's subroutine, *flbsc1*, which outputs the phases viscosities μ^p, the package provides the assumed possibility.

3.3 Numerical Results: 1D In-House Code with $flashs$

Our first step is to incorporate this ECLIPSE subroutines into described above solver. The objective is very simple: in this way, we are getting

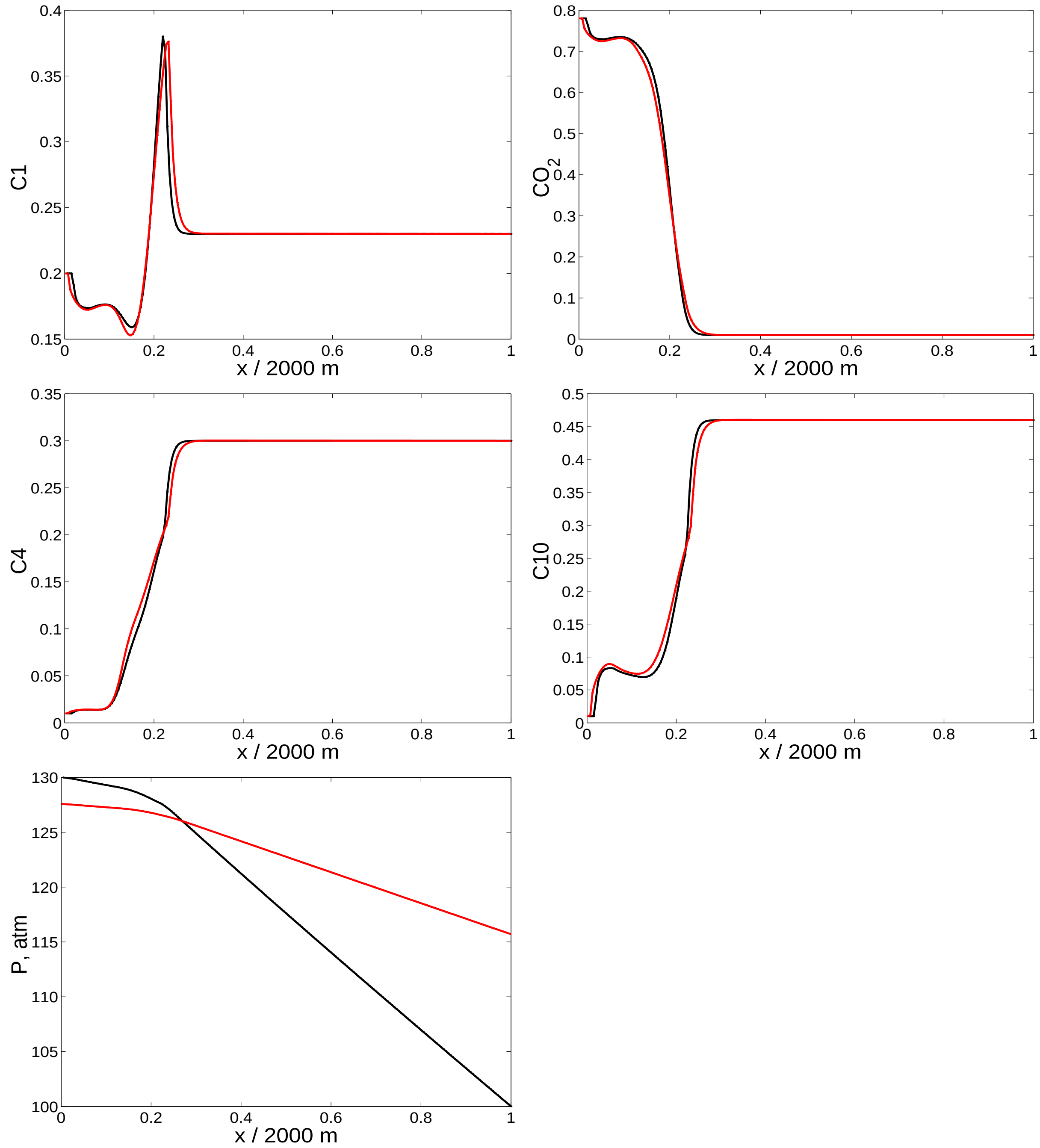

Figure 1: The results of the calculations for four-component C1-CO$_2$-C4-C10 mixture. The reservoir has initial pressure $P = 120$ atm, and temperature $T = 72^oC$. Initial concentrations of the components in the order listed are: 0.23, 0.01, 0.3 and 0.46. The injection well parameters are $P_{in} = 130$ atm, 0.2, 0.78, 0.01 and 0.01. The producing well pressure is $P_{out} = 100$ atm. Black lines show the solution obtained with Eclipse package at the moment $t = 600$ days. Red lines show the solution obtained at $t = 1600$ days with the numerical code developed in the present study where the state of the phases is determined with the help of ECLIPSE subroutines *flashs* and *flbsc1*.

a transparent experimental solver with separated pressure updating and composition updating algorithms.

Figure 1 presents the results of the simulations performed in the way described above in comparison with the results of the ECLIPSE package simulations.

Evidently, there is almost perfect coincidence between the solutions for concentration distributions generated by both codes.

As of to-day, there is a difference in pressure distributions and respective time scale between these two solutions. The reason is probably in the specification of input well parameters which we were unable to clearly identify at the moment in the Eclipse 2004A environments. In spite of this discrepancy, the results presented at Fig. 1 confirm validity of the developed code for further numerical experiments with an alternative procedure for phase state representation that constitutes a primary objective of our study.

4 Alternative Description of Phase Equilibrium

4.1 Alternative Variables (C_1, γ)

In the described above procedure, we have to calculate phase equilibrium at any spatial point and at any time step in order to obtain the values of C_i^l,C_i^g,b^l, b^g, and μ^l, μ^g. According to fundamental properties of the two-phase state of multicomponent systems, all these quantities are functions of a $(N_c - 2)$-dimensional vector-parameter $\boldsymbol{\gamma}$ of tie-lines and pressure P (see Reports [1], [2], [3]). Thus, a simple approximation of phase equilibria in terms of tie-line parameter $\boldsymbol{\gamma}$ and the leading component concentration C plays a pivotal role in our approach. The approximation used is essentially semi-empiric and is based on several observations of 'typical' behavior of real phase diagrams. This Report revisits this topic and summarizes both

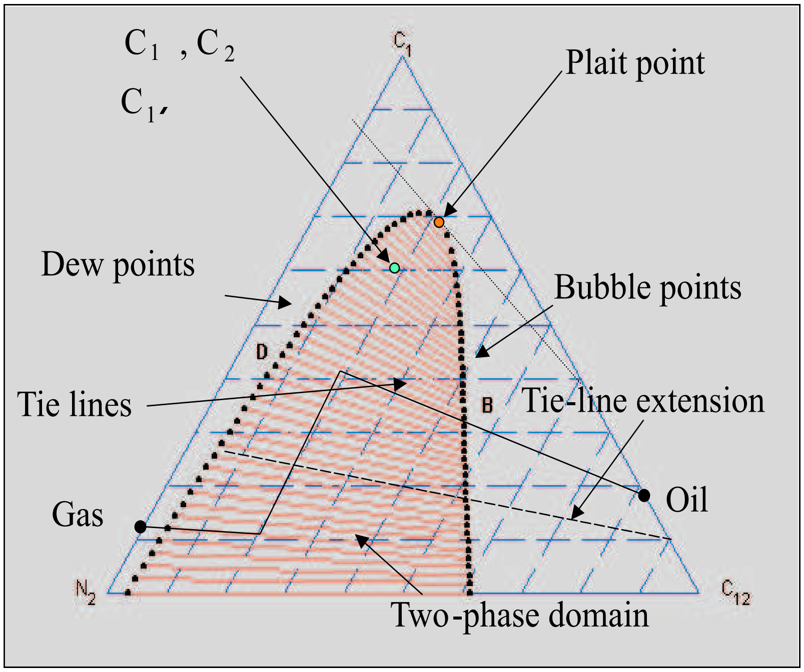

Figure 2: The phase diagram for the $C_1 - N_2 - C_{12}$ mixture at T=247^oC and $P = 170$ atm.

the approach used and some new developments.

Let us illustrate the way we introduce the tie-line vector in the case of a ternary mixture. Figure 2 shows the phase diagram for the $C_1 - N_2 - C_{12}$ mixture at T=247^oC and $P = 170$ atm.

It is well known that each composition vector of a N_c component mixture can be represented by a point within the $N_c - 1$ dimensional regular polyhedron of unit height; it is a triangle in the case under consideration. The interior of the triangle is divided into single-phase and two-phase domains. Those are separated with $N_c - 2$ dimensional binodal surface, which is the locus of bubble points and dew points.

Thermodynamics implies that there is one-to-one correspondence between the sets of bubble points and dew points. This correspondence is specified by the requirement that compositions corresponding to two respective points are in thermodynamic equilibrium. Let $\boldsymbol{C}^l$ and $\boldsymbol{C}^g$ be two such points. Then, all the compositions along the straight segment

$$\Theta : \boldsymbol{C} = \boldsymbol{C}^l L + \boldsymbol{C}^g (1 - L), \quad 0 \leq L \leq 1 \tag{15}$$

correspond to two-phase mixture of liquid of composition $\boldsymbol{C}^l$ at molar fraction L and gas of composition $\boldsymbol{C}^g$ at molar fraction $(1 - L)$. The segment Θ is a *tie-line*.

Two tie-lines do not intersect within the two-phase domain. This means that given composition breaks into a unique combination of the liquid and gaseous phases. Therefore, there exists one-to-one correspondence between any two of the three sets: the set of bubble points, the set of dew points and the set of tie lines.

Let us choose now one of components (say, the most light one) as the *leading* or *principal* component and use its concentration as the along-tie-line coordinate. Let us also consider one of components (say, the heaviest one) as the dependent one. Then, all other $N_c - 2$ components are referred to as *intermediary* ones and are used to introduce the tie-line parameter vector $\boldsymbol{\gamma}$ by the relation

$$\boldsymbol{\gamma} = \{C_2^m, ..., C_{N_c-1}^m\}, \tag{16}$$

where the superscript m denotes the midpoint of tie-line.

Note that the suggested way to introduce the alternative coordinates $(C_1, \boldsymbol{\gamma})$ is not the only one of course. It has been chosen in the cited above reports since the observations of numerous 3 and 4 component phase diagrams suggested that the following two common properties approximately hold for the diagrams:

- the binodal surfaces has parabola-like (in 2D) or paraboloid-like (in 3D) shape;

- midpoints of tie-lines are located along an almost straight line (a hyperplane in the case of multidimensional diagrams).

At the same time, some remarkable properties of the suggested change of variables has been pointed out in our previous reports, which allow us to consider the change to be rather promising for the modeling of the multicomponent two phase flows.

First of all, is has been shown that in some particular cases, namely in 1D self similar flows, the suggested change of variables makes it possible to split the problem into physico-chemical and fluid dynamical ones.

Besides, as is has been shown there as well, the suggested set of $(C_1, \boldsymbol{\gamma})$ variables allows the concise description of phase equilibrium and phase properties. In the present study we discuss how this property can be used in numerical modeling of displacement problems.

Finally, it has been supposed, that the observed property of approximate route invariance in multidimensional displacement problems would allow to construct efficient numerical codes. In the present study we discuss this topic as well.

4.2 Approximation of Phase State with Alternative Variables

To find the explicit dependence of phase state functions on new variables, a number of tie-lines should be generated at first. The scanning procedure is described in detail in previous Reports. Here we just recall that the basic idea is to start from the midpoint of the longest tie-line at the edge of phase diagram, and then proceed layer-by-layer choosing each next computational point well within the two-phase domain of the compositional space (Fig. 3). For each tie-line the flash calculations are preformed, which return the compositions of phases, their molar densities and phases viscosities.

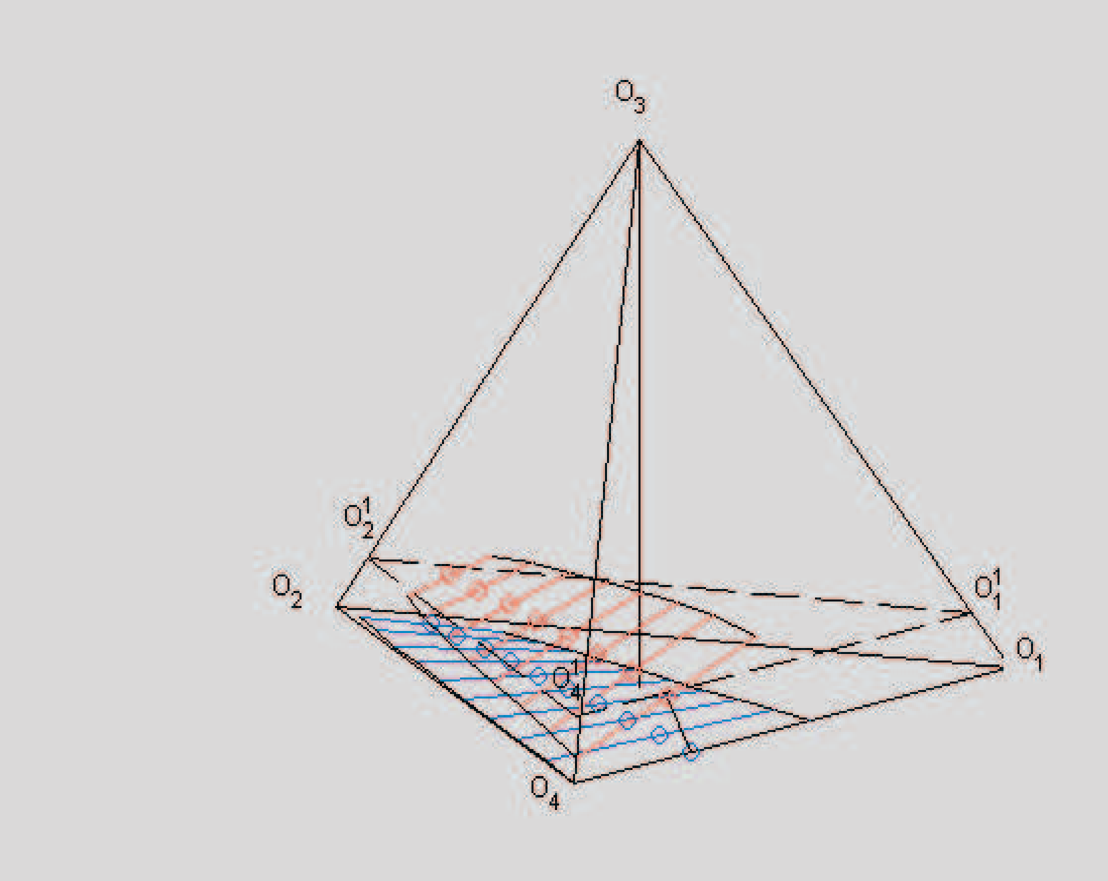

Figure 3: The schematic scanning procedure of the phase diagram for the quarternary mixture.

In the previous studies, as well as in the present one, simple expressions for composition of phases as function of $\boldsymbol{\gamma}$ are used as suggested by the observed shape of the two-phase domain.

First, the phase concentrations of the intermediary components are approximated as follows:

$$C_k^l = \gamma_{k-1} P^{(k)}(\boldsymbol{\gamma}), \quad C_k^g = 2\gamma_{k-1} - C_k^l, \quad k = 2, ..., N_c - 1 \tag{17}$$

where $P^{(k)}$ are the second order polynomials of $\boldsymbol{\gamma}$:

$$P^{(k)}(\boldsymbol{\gamma}) = \sum_{i=1}^{I_P} P_i^{(k)} \prod_{j=1}^{J_P} \gamma_j^{\alpha_{ji}}, \tag{18}$$

α being an $I_p \times J_p$ array. For example, if $N_c = 4$, $I_p = 6$, $J_p = N_c - 2 = 2$,

$$\alpha = \begin{pmatrix} 2 & 0 & 1 & 0 & 1 & 0 \\ 0 & 2 & 0 & 1 & 1 & 0 \end{pmatrix}$$

and

$$P^{(k)} = P_1^{(k)}\gamma_1^2 + P_2^{(k)}\gamma_2^2 + P_3^{(k)}\gamma_1 + P_4^{(k)}\gamma_2 + P_5^{(k)}\gamma_1\gamma_2 + P_6^{(k)}.$$

If $N_c = 5$, $I_p = 10$, $J_p = N_c - 2 = 3$,

$$\alpha = \begin{pmatrix} 2 & 0 & 0 & 1 & 0 & 0 & 1 & 1 & 0 & 0 \\ 0 & 2 & 0 & 0 & 1 & 0 & 0 & 1 & 1 & 0 \\ 0 & 0 & 2 & 0 & 0 & 1 & 1 & 0 & 1 & 0 \end{pmatrix}$$

and

$$P^{(k)} = P_1^{(k)}\gamma_1^2 + P_2^{(k)}\gamma_2^2 + P_3^{(k)}\gamma_3^2 + P_4^{(k)}\gamma_1 + P_5^{(k)}\gamma_2 + P_6^{(k)}\gamma_3 +$$
$$+ P_7^{(k)}\gamma_1\gamma_3 + P_8^{(k)}\gamma_1\gamma_2 + P_9^{(k)}\gamma_2\gamma_3 + P_{10}^{(k)}.$$

Approximation of the principal component concentration along the boundary of the two phase domain is introduced in two steps. Firstly, we introduce quadratic approximation of concentration along the median surface:

$$C_1^m = \frac{1}{2}(C_1^l + C_1^g) = P^{(m)}(\boldsymbol{\gamma}). \tag{19}$$

Next, we approximate the square of differential of phase concentrations as follows:

$$(C_1^l - C_1^g)^2 = [P^{(m)}(\boldsymbol{\gamma})]^2 P^{(d)}(\boldsymbol{\gamma}), \tag{20}$$

thus, the final expressions have the form:

$$C_1^l = \frac{1}{2}P^{(m)}\left[2 - \sqrt{P^{(d)}}\right], \quad C_1^g = \frac{1}{2}P^{(m)}\left[2 + \sqrt{P^{(d)}}\right], \tag{21}$$

where $P^{(m)}(\boldsymbol{\gamma})$ and $P^{(d)}(\boldsymbol{\gamma})$ have the form (18) and the sign at square root is chosen in such way that the difference between the compositions of the leading component in the gas and liquid phases remains positive.

Finally, for phase densities and viscosities the simplest quadratic approximations were adopted:

$$b^p = P^{(b)}(\boldsymbol{\gamma}), \quad \mu^p = P^{(\mu)}(\boldsymbol{\gamma}). \tag{22}$$

All polynomials have the same form and differ only by their coefficients which were evaluated using the least mean square procedure. The described above quasi-quadratic approximate procedure has been tested against available data for a number of reservoir system. Some examples of the approximation are shown in Fig.4. The compositions of phases for the 4-component mixture, obtained by standard ECLIPSE flash calculations, are shown in Fig.4 by red points, while the approximate functions are shown in blue. Yellow points show the parametric domain in the tie-line parameter (γ) space. One can see, that the quasi–quadratic approximation of phase compositions can be considered as good enough everywhere excluding the very close vicinity of the plait point. At the same time, the simplest quadratic approximation of phase densities and viscosities is not so good but both in previous and in the present study we did not care about this too much. The reason is that we supposed that such rough approximation of these functions was good enough for the displacement problems, and, secondly we do not need, in fact, in the approximated values since ECLIPSE package allows an user to calculate these values explicitly using the special subroutines ($dlbce1$ and $dcdenu$ for phase viscosity and density respectively), with pressure, temperature and the pre-calculated values of phase compositions as input data.

4.3 Fast Transformation to Alternative Variables ($FTAV$)

In order to complete transformation to new coordinates in composition space we need a rule how to calculate the alternative variables if the stan-

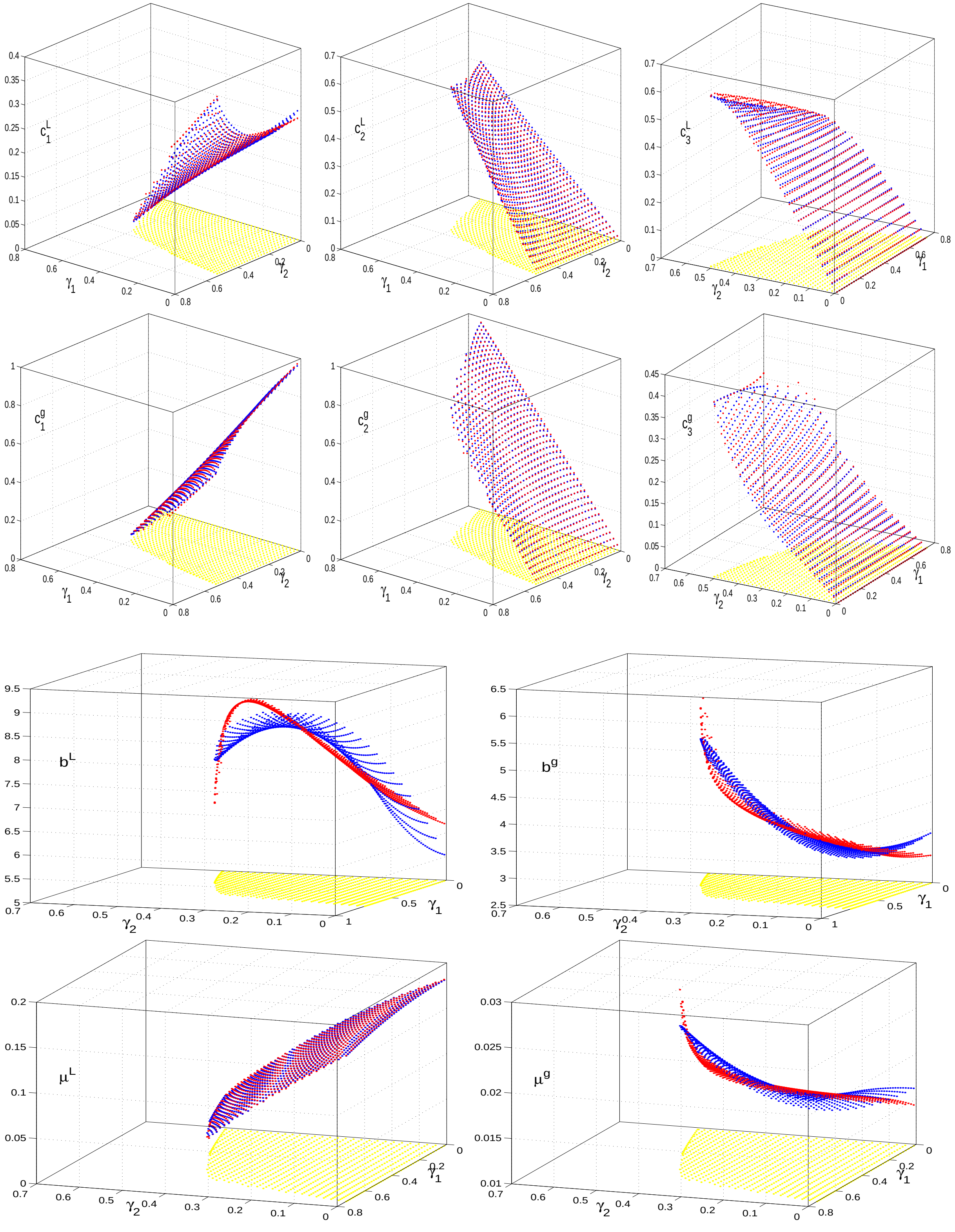

Figure 4: Approximation of phase compositions, phase densities and viscosities for the $C1-CO_2-C4-C10$ mixture at $T = 72C$ and $P = 120$ atm.

dard ones are known and vice versa, or, in other words, to write out explicitly the tie-line equation.

Since along the tie-line the two-phase mixture composition depends on of liquid phase fraction linearly, one can obtain the dependence of the liquid fraction on the leading component concentrations in the mixture and the both phases:

$$L = \frac{C_1 - C_1^l}{C_1^g - C_1^l}. \tag{23}$$

Simple algebraic manipulations allow then to obtain the relations between concentrations of the intermediary components, the leading component, and the corresponding phase compositions as follows:

$$C_k = A_k(\boldsymbol{\gamma}, P)C_1 + B_k(\boldsymbol{\gamma}, P), \quad k = 2, ..., N_c - 1; \tag{24}$$

$$A_k = \frac{C_k^l - C_k^g}{C_1^l - C_1^g}, \quad B_k = C_k^g - A_k C_1^g. \tag{25}$$

For given phase diagram, with fixed pressure and temperature values, the phase compositions (as well as the phase densities and viscosities) depend on the tie-line vector parameter only,

$$C_k^p = C_k^p\left(\boldsymbol{\gamma}\right), \quad b^p = b^p\left(\boldsymbol{\gamma}\right), \quad \mu^p = \mu^p\left(\boldsymbol{\gamma}\right), \tag{26}$$

and, therefore, Eqs. (24) and (25) define a nonlinear relation between the standard and alternative variables.

In accordance with equations (25), (17) and (21) the explicit dependence of the coefficients A_k and B_k on $\boldsymbol{\gamma}$ can be written as follows:

$$A_k = -2\frac{\gamma_{k-1}\left(P^{(k)} - 1\right)}{P^{(m)}\sqrt{P^{(d)}}}, \quad B_k = \gamma_{k-1}\left(1 + 2\frac{P^{(k)} - 1}{\sqrt{P^{(d)}}}\right). \tag{27}$$

One can see in Fig. 5, that described in the previous subsection approximative procedure gives the perfect result for the A_k and B_k functions as well.

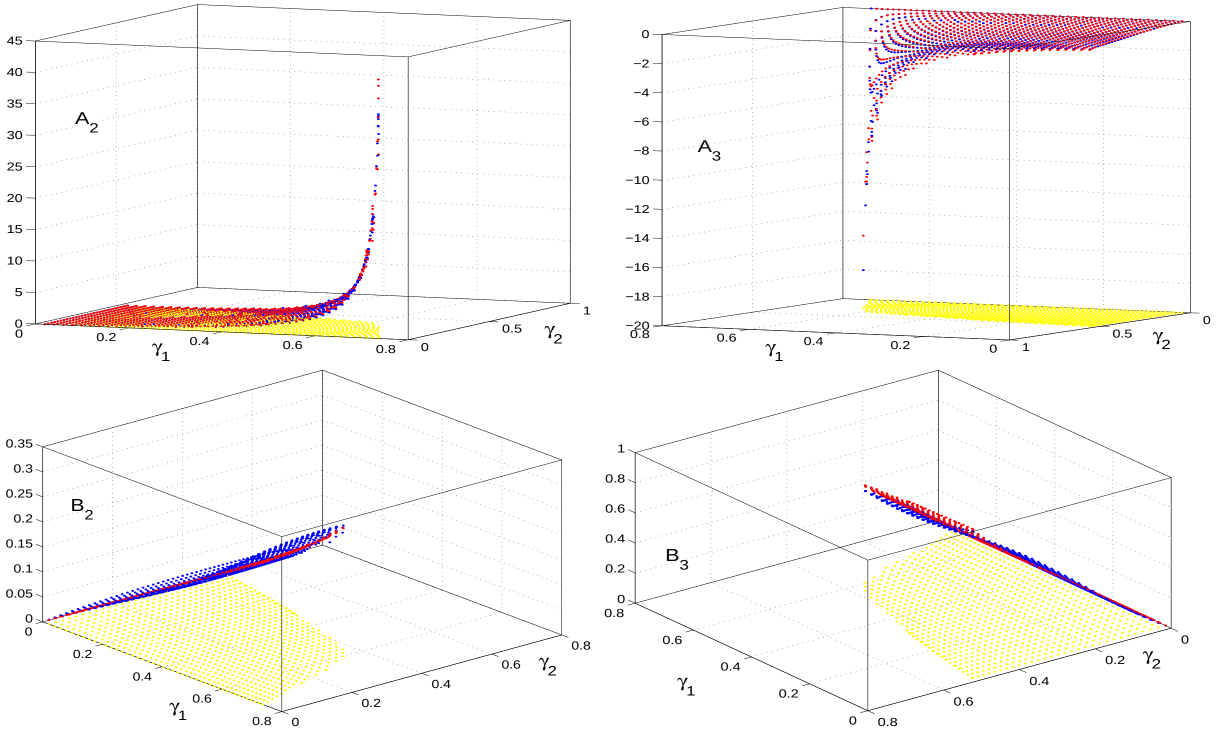

Figure 5: Approximation of A_k and B_k functions for the $C1 - CO_2 - C4 - C10$ mixture at $T = 72C$ and $P = 120\ atm$.

A key point in the algorithm being developed is to find values of the alternative variables $\boldsymbol{\gamma}$ provided that the overall composition $\boldsymbol{C}$ is specified, or to solve the system of equations (24). It can be written in the form:

$$f_1 = 2\gamma_1 \left(P^{(2)} - 1\right) C_1 + GC_2 - \gamma_1 \left(G + 2P^m \left(P^{(2)} - 1\right)\right) = 0;$$

$$f_i = 2\gamma_i \left(P^{(i+1)} - 1\right) C_1 + GC_{i+1} - \gamma_i \left(G + 2P^m \left(P^{(i+1)} - 1\right)\right) = 0;$$

$$\ldots. \tag{28}$$

$$f_{J_p} = 2\gamma_{J_p} \left(P^{(J_p+1)} - 1\right) C_1 + GC_{J_p+1} - \gamma_{J_p} \left(G + 2P^m \left(P^{(J_p+1)} - 1\right)\right) = 0;$$

where $G = P^m\sqrt{P^d}$. This procedure has been developed anew, following completely different than before, while quite straightforward algorithm based on the Newton method. First, we evaluate the Jacobian matrix

$$J_{ij} = \frac{\partial f_i}{\partial \gamma_j},$$

and then iterate the system starting with an initial value $\boldsymbol{\gamma}_0$. After simple calculations we have:

$$\frac{\partial f_i}{\partial \gamma_i} = 2\gamma_i \left(C_1 - P^m\right) \frac{\partial P^{(i+1)}}{\partial \gamma_i} + \left(C_{i+1} - \gamma_i\right) \frac{\partial G}{\partial \gamma_i} + 2\gamma_i \left(1 - P^{(i+1)}\right) \frac{\partial P^m}{\partial \gamma_i} + \\ +2P^m - G + \left(2C_1 - 2P^m\right) P^{(i+1)} - 2C_1,$$

and

$$\frac{\partial f_i}{\partial \gamma_j} = 2\gamma_i \left(C_1 - P^m\right) \frac{\partial P^{(i+1)}}{\partial \gamma_j} + \left(C_{i+1} - \gamma_i\right) \frac{\partial G}{\partial \gamma_j} + 2\gamma_i \left(1 - P^{(i+1)}\right) \frac{\partial P^m}{\partial \gamma_j};$$

with

$$\frac{\partial P}{\partial \gamma_k} = \sum_{i=1}^{I_P} P_i^{(z)} \frac{\partial}{\partial \gamma_k} \prod_{j=1}^{J_P} \gamma_j^{\alpha_{ji}} = \sum_{i=1}^{I_P} P_i^{(z)} \alpha_{k,i} \gamma_k^{-1} \prod_{j=1}^{J_P} \gamma_j^{\alpha_{ji}},$$

$$\frac{\partial G}{\partial \gamma_k} = \frac{\partial P^m \sqrt{P^d}}{\partial \gamma_k} = P^m \frac{\partial \sqrt{P^d}}{\partial \gamma_k} + \sqrt{P^d} \frac{\partial P^m}{\partial \gamma_k} = \frac{P^m}{2\sqrt{P^d}} \frac{\partial P^d}{\partial \gamma_k} + \sqrt{P^d} \frac{\partial P^m}{\partial \gamma_k}.$$

Now, following the Newton method, we have

$$\mathbf{f}\left(\boldsymbol{\gamma}^{n+1}\right) = \mathbf{f}\left(\boldsymbol{\gamma}^n + \Delta\boldsymbol{\gamma}\right) = \mathbf{f}\left(\boldsymbol{\gamma}^n\right) + \Delta\boldsymbol{\gamma} \cdot \frac{\partial \mathbf{f}}{\partial \boldsymbol{\gamma}}\left(\boldsymbol{\gamma}^n\right) = 0$$

and, therefore,

$$\Delta\boldsymbol{\gamma} = -\left[\frac{\partial \mathbf{f}}{\partial \boldsymbol{\gamma}}\right]^{-1} \cdot \mathbf{f}.$$

Surprisingly enough, it turned out, that the choice

$$\boldsymbol{\gamma}_0 = 0 \tag{29}$$

proved to be the best (at least for $N_c \leq 5$) in the sense that the Newton iterations converge rapidly (3-4 iterations) to attain the relative accuracy 10^{-8}.

As a result, we now have a technique for fast transformation from $\boldsymbol{C}$ to $\boldsymbol{\gamma}, C$ variables and back.

It allows us to convert the described above in-house simulator into a prototype alternative simulator (ALTSIM-2) in which all phase equilibria are expressed in terms of the alternative state variables $\boldsymbol{\gamma}$ and C.

4.4 Numerical Results: 1D In-House Code with $FTAV$

Let us now return to the first objective of this Project, namely to construction of alternative 1D code for displacement problem. The code will be based on the developed above γ-approximation of phase equilibrium and the developed technique which allows to perform fast transformation from standard $\boldsymbol{C}$ variables to alternative $(C_1, \boldsymbol{\gamma})$ variables and vice versa.

We recall now, that the first step in this Project was development of 1D simulator where the thermodynamic state of the phases was specified with the help of ECLIPSE's flash subroutines. We have shown by comparison with the standard ECLIPSE code the validity of the code to solve the displacement problems.

The drawback of that code, as we believe, is that we have to calculate phase equilibrium at any space point and at any time step. The external approximation of phase equilibria based on $(C_1, \boldsymbol{\gamma})$ variables makes it possible now to take the flash procedure outside the computational loop.

To illustrate this idea, let as look again at the general structure of the numerical algorithm described in Sect. 3.1. As it was suggested there, at each time step and at each iteration we obtain the values of pressure P^q and concentrations of components $\boldsymbol{C}^q$ by solving the system of governing equations, which are written in terms of standard $\boldsymbol{C}$ variables.

It is possible then, using the found values P^q and $\boldsymbol{C}^q$, to determine functions $(C_k^p)^q$, $(b^p)^q$, $(\mu^p)^q$ in accordance with equations of state (4). Instead of the standard ECLIPSE's subrotines $flashs$ and $flbsc$ which were used for this purpose in Sect. 3.2, we make now the change of variables at each space point, using the fast transformation technique described above. We determine all component phase concentrations, phase densities and viscosities as functions of $\boldsymbol{\gamma}$ using the interpolated beforehand data, where

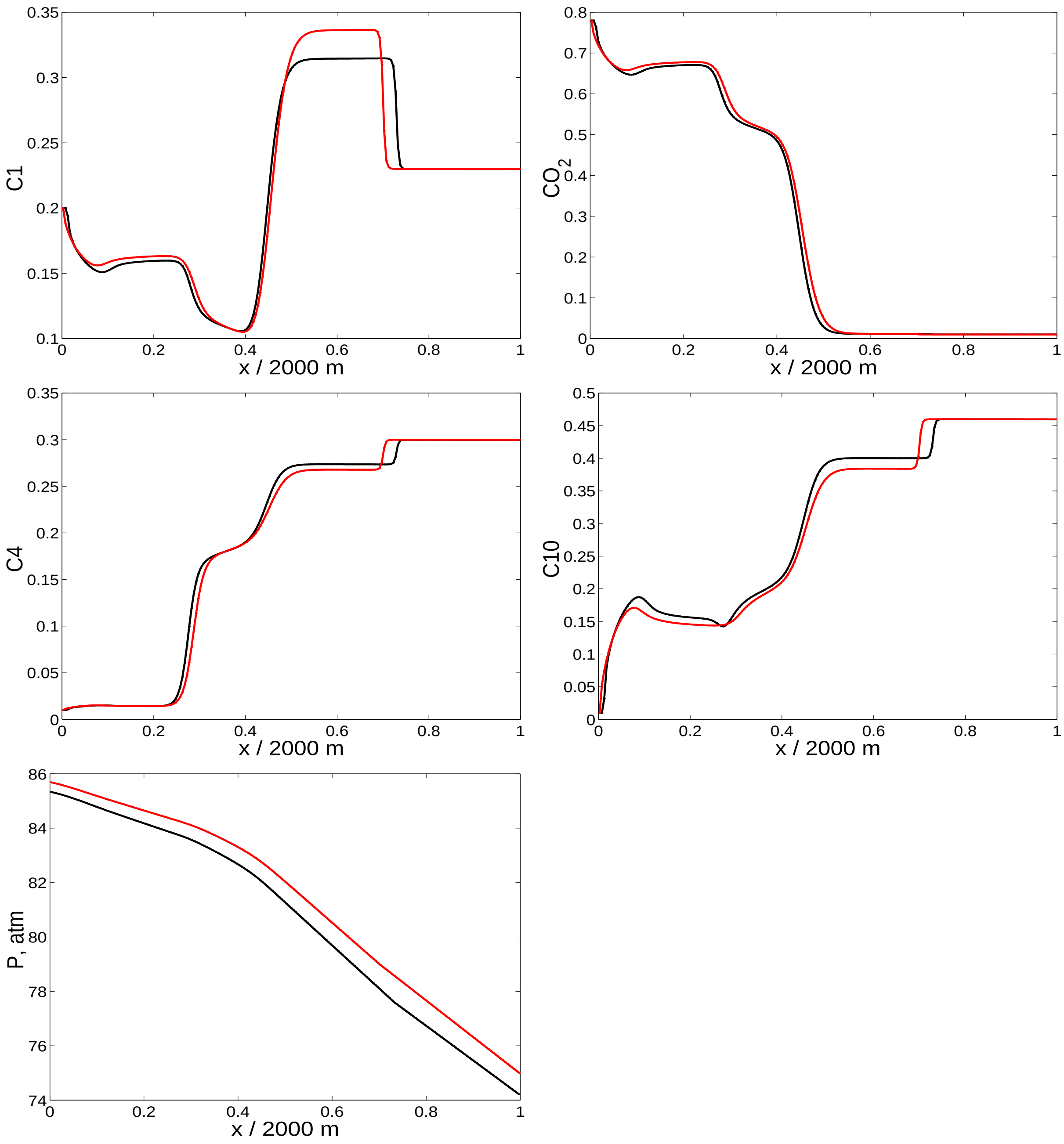

Figure 6: The results of the calculation for four-component C1-CO$_2$-C4-C10 mixture. The reservoir has initial pressure $P = 85$ atm, the reservoir temperature $T = 93^o$. Initial concentrations of the components in the order listed are: 0.23, 0.01, 0.3 and 0.46. The injection well parameters are $P_{in} = 90$ atm, 0.2, 0.78, 0.01 and 0.01. The producing well pressure is $P_{out} = 60$ atm. Black lines represent the solution obtained with the help of developed 1D in-house code with $FTAV$ procedure at the moment $t = 1800$ days. Red lines represent the solution obtained at $t = 2000$ with the numerical code developed in the present study where the state of the phases is determined with the help of ECLIPSE subroutines *flashs* and *flbsc1*.

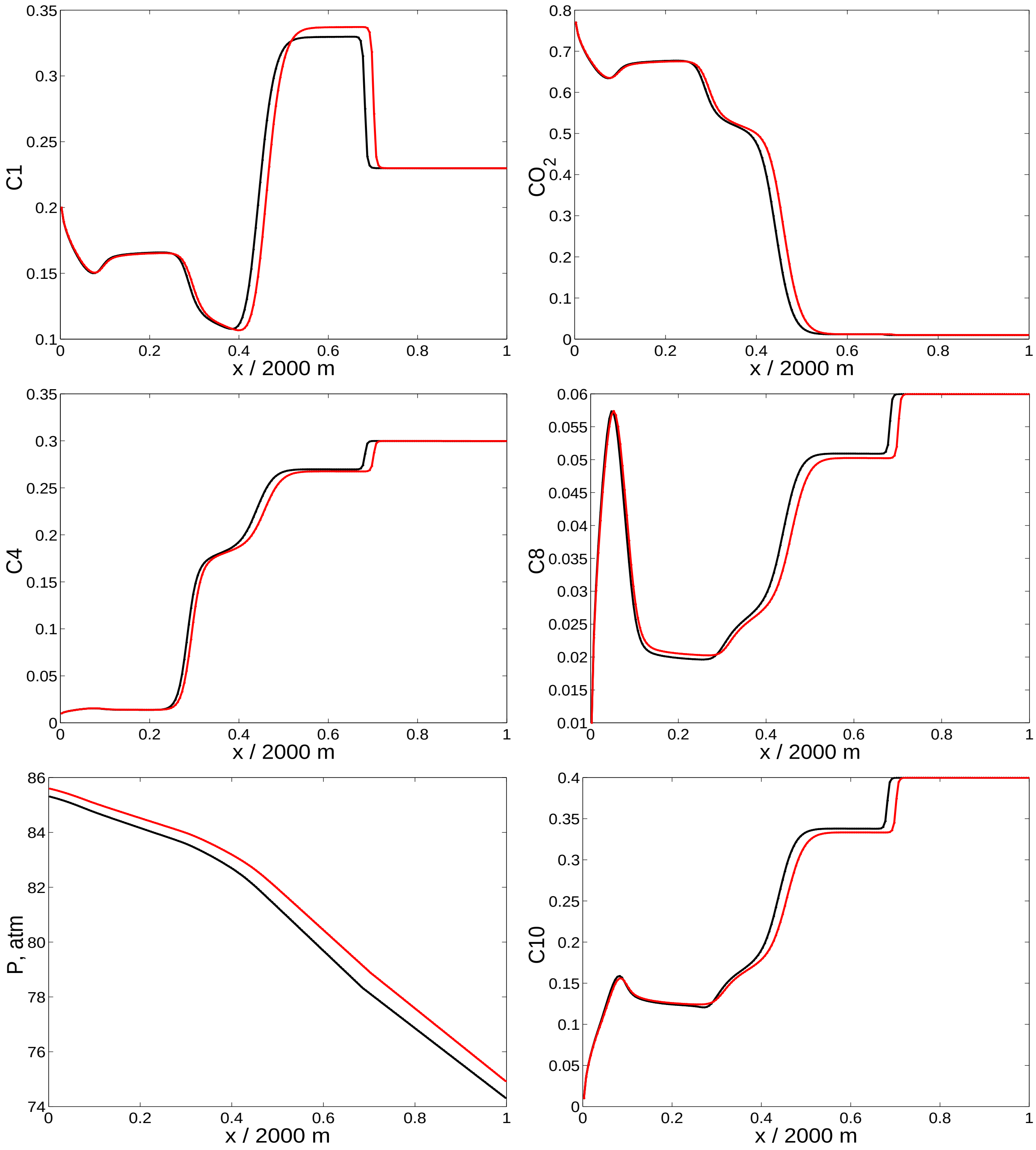

Figure 7: The results of the calculation for the five component C1-CO_2-C4-C8-C10 mixture. The reservoir has initial pressure $P = 85$ atm, the reservoir temperature $T = 93^o$. Initial concentrations of the components in the order listed are: 0.23, 0.01, 0.3, 0.4 and 0.06. The injection well parameters are $P_{in} = 90$ atm, 0.2, 0.77, 0.01, 0.01 and 0.01. The producing well pressure is $P_{out} = 60$ atm. Black lines represent the solution obtained with the γ parametrization at the moment $t = 1800$ days. Red lines represent the solution obtained at $t = 2000$ with the numerical code developed in the present study where the state of the phases is determined with the help of ECLIPSE subroutines *flashs* and *flbsc1*.

the polynomial coefficients $P_i^{(k)}$, $P_i^{(m)}$, $P_i^{(d)}$, $P_i^{(b)}$ and $P_i^{(\mu)}$ (see Sect. 4) are stored in the memory and do not change during calculations. It should be noted here, that the approximation procedure has been performed for a fixed value of pressure, while it may change during calculations. However, it has been shown in the previous reports, that in wide enough pressure range it is possible to consider the coefficients as pressure-independent, or as linear functions of pressure. Respective modifications of the codes developed can be introduced straightforwardly.

Thus, at each time step and at each iteration we translate the updated values of concentrations into updated values of fluid-dynamics related variables (such as phase compositions, densities viscosities, saturations). With these values we evaluate new values of pressure and concentrations and repeat the cycle. In a sense, we now working simultaneously in two sets of variables. As a result, we make change of variables not once and forever, as has been suggested in the previous reports, but at each time step and at each spatial point. This pragmatic approach, while not necessarily being the best choice, makes it possible to keep intact entire computational infrastructure of ECLIPSE, and makes transition to new variables much less painful.

To demonstrate efficiency of the described above numerical procedure, we run the simulation similar to that, presented in Fig. 1, but for a little different pressure and temperature values. The results are shown in Figs. 6, 7. One can see again the perfect coincidence between the results of our $\boldsymbol{\gamma}$ and *flashs* solvers. A small delay in time is related to non-perfect approximation of the phase molar densities and viscosities (we checked this by additional runs where the mentioned variables only were calculated by *flashs* solver). What is important in this demonstration, is the

CPU time needed to attain the same moment of physical time in different solvers. This feature is about 20 times less for the $\boldsymbol{\gamma}$ solver when compared with our *flashs* solver. Since both solvers differ only in the part related to the phase state calculation, one may expect that, being inserted into the Eclipse package, our $\boldsymbol{\gamma}$ solver will save the similar amount of the CPU time. We return to this topic in Sect. 6.

5 Route Invariance and its Numerical Implications

5.1 Route Definition

As it has been noted in Sect. 4, another remarkable property of the alternative variables $C_1, \boldsymbol{\gamma}$ is the experimentally observed property of approximate *route invariance* for the problems of oil displacement by gas injection.

This Section is devoted therefore to study of this property, which eventually is becoming more and more important for two-phase multicomponent flows. To begin with, we remind some definitions and basic facts.

Consider a flow of a multicomponent system characterized by time dependent composition fields: $\boldsymbol{C}(\mathbf{x}, t)$. The same distributions can be equivalently characterized by the fields of alternative variables $C_1(\mathbf{x}, t), \boldsymbol{\gamma}(\mathbf{x}, t)$. In particular, if we are using a kind of standard reservoir simulator such as ECLIPSE, the output directly provides sets of concentrations $C_k^g(x, t)$, $C_k^l(x, t)$ in the grid points. Therefore if we define tie-line vector as above, then we directly have fields of $\gamma_i = 0.5(C_{k+1}^g + C_{k+1}^l)$, $k = 1, \ldots, N_c - 2$. Now we define the *route* in $\boldsymbol{\gamma}$-space as the locus of points $\gamma_1, \gamma_2, \ldots \gamma_{N_c-2}$ space for fixed time t. (If our spatial grid consists of I_{max} points, the route also consists of I_{max} points, some of which may coincide.) It characterizes the set of tie lines 'active' at given time. It is convenient to consider the discrete point set as a representation of a continuous curve. In general, the

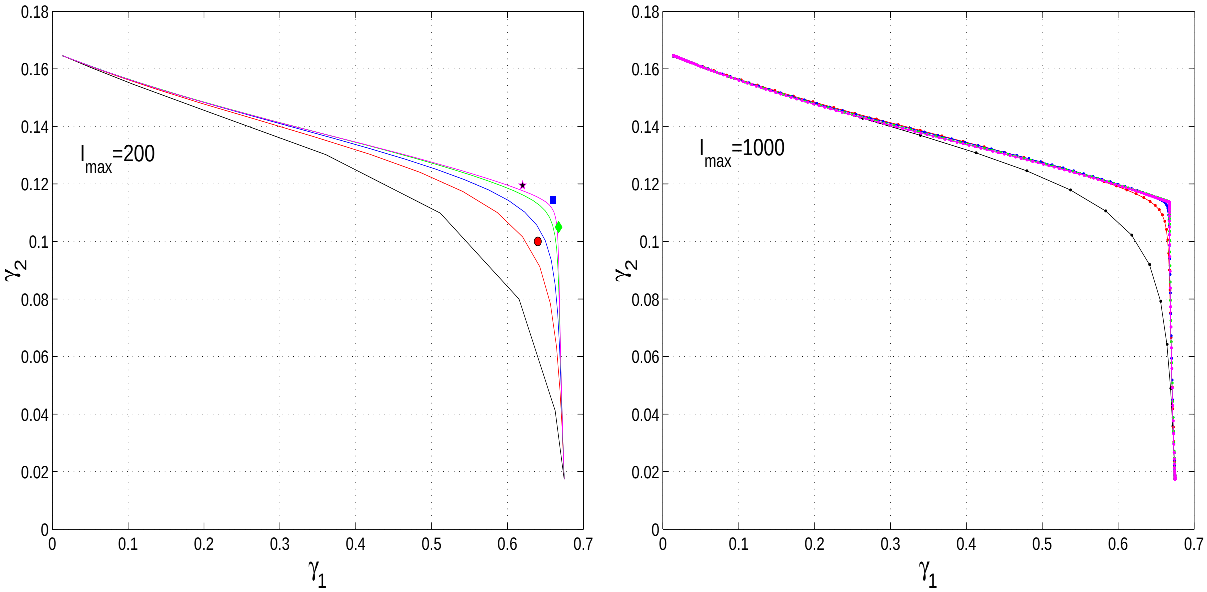

Figure 8: Route in $\boldsymbol{\gamma}$ space for different moments of time for the solutions of oil displacement problems obtained with different grid resolution. The input/output conditions and the reservoir parameters are the same as in Fig. 1. Black, red, blue, green and magenta lines correspond to the time moments 100, 500, 1000, 2000 and 3000 days respectively. Note that on grid with higher resolution the routes are different only at the early stage of the flow evolution. The colored symbols in the left panel indicate the position of the middle point of considered further different three-point quasi-linear approximation of the limiting time independent route. The other two points in such approximation are not indicated in the Figure since their choice is obvious.

route evolves in time.

5.2 Route Invariance in 1D and 2D Displacement Flows

An important theoretical result consists in that for similarity solution of the Riemann problem corresponding to oil displacement by continuous injection of gas mixture at negligible pressure differential the route does not depend on time, or is *invariant*. In this case, the route is evidently a continuous curve. More than that, the route is also invariant in another sense, namely, it does not depend on flow properties, such as relative permeabilities and phase viscosities, and is determined completely by the system phase behavior and two values of the tie-line parameter corresponding to oil

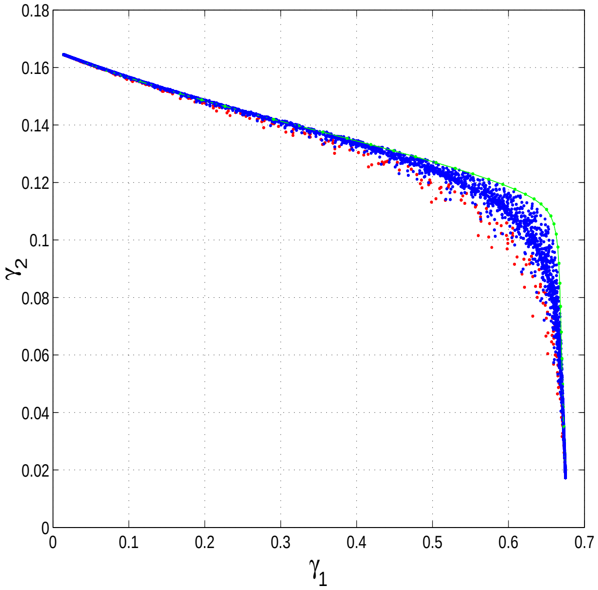

Figure 9: Route in γ space for different moments of time for the solutions of 2D oil displacement problems obtained with different grid resolution (solution on grid 20×20 is presented by red points, on grid 40×40 – by blue points) vs. 1D time-independent route (green points, $I_{max} = 200$). The input/output conditions and the reservoir parameters are the same as in Fig. 1.

in place and the injected gas mixture. In principle, the route can be found as solution of an auxiliary Riemann problem stated completely in terms of properties related to phase equilibrium of a mixture of given components.

In reservoir simulations of oil displacement by injection of gas mixtures can not be considered strictly as a self similar flow, due to variable pressure and effects of numerical dispersion. However, it has been experimentally established that an approximate route invariance holds there as well.

This feature is illustrated in Fig. 8, where the routes are shown for the displacement problem with inflow/outflow conditions and reservoir parameters being the same as in Fig. 1. One can see that the routes corresponding to different times are spread out in the γ space, but with time they tend to a single limiting route the faster the higher the grid resolution.

Another important property of the route is the experementally observed fact, that in 2D displacement problems route at not too large times approaches with time to the same time-independent route as in correspondineg 1D flow. Fig. 9 presents the routes in 2D displacement problem obtained with the help of 2D in-house simulator (see Sect. 3.1) on the 20×20 grid (red points), 40×40 grid (blue points) and the 1D time-independent route (green points, $I_{max} = 200$).

5.3 Numerical Code Based on Route Invariance Property (RIP–technique)

The approximate route invariance property makes it possible to develop an version of the alternative numerical code for solution of 1D oil displacement problem as follows. The idea is based on the direct application of this property to reduce modeling of a multicomponent flow to an effectively two-component one. Suppose that the limiting time independent route for a N_c component displacement problem is known, and this route is a segment of a continious curve in $N_c - 2$ dimensional $\boldsymbol{\gamma}$ space. The segment can be parametrized somehow, for example by its length s. Thus, the values

$$\boldsymbol{\gamma}(s) = \{\gamma_1(s), \dots, \gamma_{N_c}(s)\}$$

are known at any spatial point and at any moment of time if the value of s is known there.

The values of phase compositions, phase densities and viscosities, as well as of functions A_k and B_k can be therefore determined as well (see Sect. 4). If, in addition, the values of pressure P and the leading component concentration C_1 are known as well, the solution at given spatial and temporal point can be completely reconstructed with the help of relation (24) which we rewrite here again for the sake of convenience:

$$C_k = A_k(s)C_1 + B_k(s), \quad k = 2, ..., N_c - 1. \tag{30}$$

To solve the multicomponent displacement problem we have to solve therefore three equations of the system (1):

$$\begin{aligned}
&\frac{\partial mb}{\partial t} + div\left(\mathbf{U}^l b^l(s) + \mathbf{U}^g b^g(s)\right) + Q = 0;\\
&\frac{\partial mbC_1}{\partial t} + div\left(\mathbf{U}^l b^l(s) C_1^l(s) + \mathbf{U}^g b^g(s) C_1^g(s)\right) + q_1 = 0;\\
&\frac{\partial mbC_2}{\partial t} + div\left(\mathbf{U}^l b^l(s) C_2^l(s) + \mathbf{U}^g b^g(s) C_2^g(s)\right) + q_2 = 0.
\end{aligned} \tag{31}$$

where subscript $'1'$ corresponds to the chosen beforehand leading component, and subscript $'2'$ – to any other component of the $N_c > 3$ component mixture. Since C_2 in accordance with the relations (30) can be considered as a function of s, the system (31) is a closed system of p.d.e. for b,C_1 and s.

This system is not, however, resolved with respect to the time derivatives and that is why we consider C_2 as the independent unknown variable when solve the system (31) in the present study. In more detail, let us suppose that the solution in all spatial points at a moment of time is known. That means, that we know all phase compositions, densities and viscositities. thus, we can determine the values of C_1 and C_2 at next time step (or iteration) by solving the system (31). Then, with the help of the nonlinear equation (30) with $k = 2$ we can obtain the value of parameter s. Then, as it has been already described above, we can recover the values of $\boldsymbol{\gamma}$, which, in turn, with the help of the stored beforehand in the memory polynomial coefficients, can be used for the reconstruction of the phase compositions at the next time step (or iteration), and, at the same, for the reconstruction of the values of concentrations of the rest components with the help of relations (30) with $k = 3, \ldots, N_c - 1$.

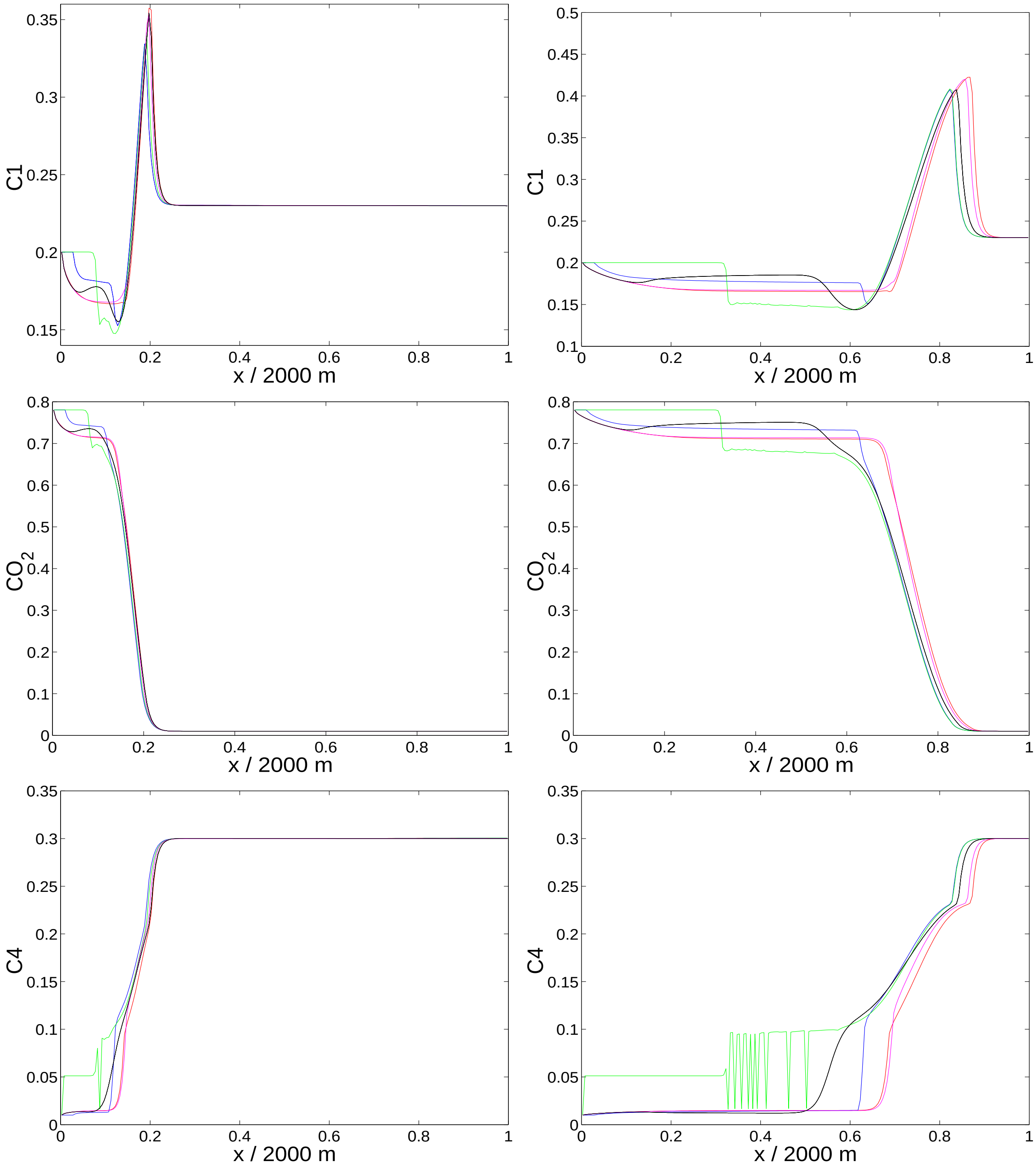

Figure 10: The results of the 1D RIP calculations for four component C1-CO$_2$-C4-C10 mixture. The input/output conditions and the reservoir parameters are the same as in Fig. 1. The results in the left column correspond to $t = 1000$ days, in the right – to $t = 4000$ days. Red, blue, green and magenta lines correspond to different three-point quasi-linear approximations of the limiting time-independent route. The color of the line corresponds to the color of the symbol in the left panel of Fig. 8. Black lines present the 'correct' solution, obtained in ALTSIM-2 simulations (see Sect. 4.4).

5.4 Numerical Results: 1D RIP simulations

To test the suggested technique (hereafter *Route Invariance Property* (RIP) technique), we consider the four component 1D displacement problem, results for which were presented in Figs. 1 and 8. Keeping the value $I_{max} = 200$ and $C1$ as the leading component, we choose CO_2 as the second component in the pseudo three-component system, and $C4$ as the third component. That means that subrsripts '1' and '2' in notations of the system (31) refer to $C1$ and CO_2 respectively, the molar concentration of $C4$ is reconstructed with the help of (30), and $C10$ is considered as dependent component.

We have run a series of simulations which differ one from another by the chosen position of the middle point in a three point quasi-linear approximation of the limiting time-independent poute (see colored symbols n the left panel of Fig. 8).

The results of the 1D RIP calculations for four component mixture at different moments of time are presented in Fig. 10. Red, blue, green and magenta lines there correspond to different three-point quasi-linear approximations of the limiting time-independent route. The color of each line corresponds to the color of the symbol in the left panel of Fig. 8. Black lines present the 'correct' solution, obtained in ALTSIM-2 simulations (see Sect. 4.4). As could be expected, the blue lines are closer to the correct solution since the blue square gives the best approximation of the route. At the same time, other colors give the acceptable approximation of the correct solution, excluding oscillating results presented by the green lines. Interestingly enough, that red and magenta lines in Fig. 10 practically coincide, although the corresponding symbols in Fig. 8 are far enough.

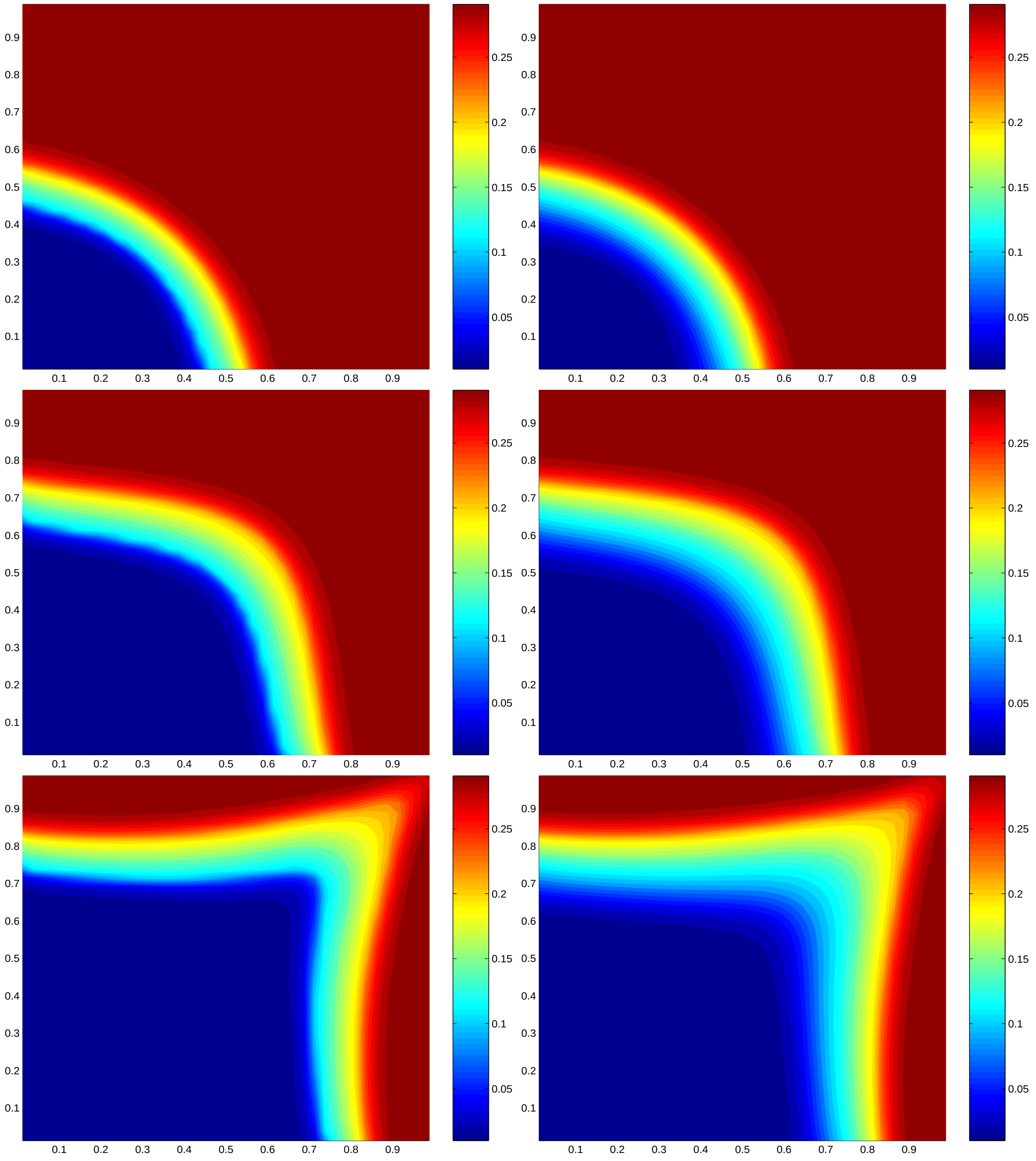

Figure 11: The results of the 2D RIP calculations for four component C1-CO_2-C4-C10 mixture (left column) vs. 2D ALTSIM-2 simulations (right column). $C4$ distributions are presented. The input/output conditions and the reservoir parameters are the same as in Fig. 1. The results in the upper row correspond to $t = 2500$ days, in the middle – to $t = 5000$ days, in the lower – to $t = 7500$ days. The three-point quasi-linear approximations of the 1D limiting time-independent route correspond to the magenta pentagon (Fig. 8).

5.5 Numerical Results: 2D RIP simulations

Property of route invariance can be in principle used to improve performance of 2D compositional simulators as well. The idea is based again on the mentioned above experementally observed fact, that route distribution in 2D displacement problem with time tends to the same time-independent route as in correspondineg 1D flow. Thus, if the 1D limiting time-independent route is known, say, from 1D calculations, the RIP technique can be applied in 2D case in the exactly the same way as described above in 1D case. The results of the test calculations are shown in Fig. 11. One can observe good enough coincidence with the 2D ALTSIM-2 simulation results in the distribution at different moments of time, including the moment of gas breakthrough.

6 Incoporation into ECLIPSE

The ultimate objective of this work is to develop a version of ECLIPSE based on an alternative representation of phase equilibrium avoiding iterative use of the flash-calculation procedure. Above we developed two alternative techniques. The first one – $FTAV$ – is based on the taking the standard flash procedure outside the displacement problem solution. We have tested this approach in our in-house 1D package and found 20 times improvemement in CPU time of $FTAV$ when compared with $flashs$. In this section we check whether the ECLIPSE 300 with $FTAV$ incorporated into it still demonstrates such improvement when compared with its standard version. The second alternative technique – RIP technique – essentially uses the experementally established route invariance property. Above, the technique has been tested for the four component mixtures only. Thus, we do not have a goal now to check the technique efficiency, but just want to see whether it works being incorporated into ECLIPSE.

In the case of satisfactory result, extension of this procedure on the multicomponent case can be straightforwadly done later.

6.1 ECLIPSE with $FTAV$

The structure of ECLIPSE package is similar to the structure of the developed above in-house code.

Namely, in both codes the flash calculation is inside an iterative procedure which solves the system of conservation laws. That makes it possible to insert any alternative approximation of phase equilibria into ECLIPSE in a way similar to that used in our in-house code. Namely, as soon as the iterated values are defined, the flash-calculation procedure in the ECLIPSE should be replaced by an alternative subroutine.

After studying in detail the ECLIPSE structure it has been found that the new alternative subroutine should be inserted instead of $flashv$. The function $flashv$ built in the current version of Eclipse package is much more complicated that $flashs$ subroutine which we used to test our alternative solver. The function $flashv$ built in Eclipse outputs 30 parameters. It is necessary to replace all of them with ones calculated by the alternative block ($altFTAV$-block). Those are:

- total molar density SMT;
- total mole fractions SZ;
- liquid mole fraction SL;
- vapour mole fraction SV;
- K-values SK and $SJ = \log SK$;

- component liquid SX and vapour SY mole fractions;
- liquid SZL and vapour SZV z-factors;
- z-factors derivatives with respect to pressure $SZLP$, $SZVP$;
- z-factors derivatives with respect to mole fractions $SZLX$ or $SZVY$;
- Jacobian matrices $SDDZ$ and $WCDZ$;
- liquid and vapour AIJ-coefficients AIL and AIV;
- BI-coefficient BI;
- state indicator array $ISIA$.

The $altFTAV$-block uses only the component molar densities from Eclipse and the coefficients of the approximating polynomials which are calculated earlier using separate program package to determine phase fractions parameters. The other parameters are determined with the help of standard Eclipse functions, inserted in the block. The structure of this block can be briefly described as follows:

1. Polynomial coefficients $P_i^{(k)}$, $P_i^{(m)}$, $P_i^{(d)}$, $P_i^{(b)}$ and $P_i^{(\mu)}$ (see Sect. 4) are read from the hard disk in the beginning of the run, stored in the memory and do not change during calculations.
2. The total mole fractions SZ are calculated from the given values of molar densities at each iteration in each spatial point.
3. At each iteration at each time step loop through cells then starts. During the loop the following procedures are performed:

   a) function *cresh* defines γ_1 and γ_2 from the known values of SZ;

   b) function *cthrmd* determines then component liquid and vapour mole fractions SX and SY

c) Then the liquid molar fraction is determined by the given values of SZ, SX and SY. Then SX and SY are updated in single phase areas.

4. After the loop through the cells, the Eclipse storage arrays are filled in by the *alt*-block variables SZ, SX and SY;
5. Finally, *cparm* subroutine is called, which is, in fact, the combinaton of standard Eclipse procedures, and has the objective to fill the rest of $flashv$ output parameters in the Eclipse storage arrays.

It has been done successfully and some experiments have been carried out. The calculations were run for the 1D flow of four-component mixture, with the same the input/output conditions and reservoir parameters as in Fig.1. Different grids were considered in the simulations: 200 cells, 600 cells and 1000 cells.

Good coincidence of these solutions is obvious from Fig. 12, where blue lines show the solution obtained with modified ECLIPSE package with the *alt*-block, and red lines correspond to standard ECLIPSE $flashv$ solution. Thus it can be concluded that *alt*-block replaced $flashv$ properly. Then it is sensible to compare the work times. We recall that it was expected that *alt*-block should be much more faster then $flashv$.

Unfortunatelly, as of to-day, that is not the case. Table 1 summarises the measured time of the modified by the *alt*-block ECLIPSE vs. its standard version. Two characteristics were considered to estimate the calculations efficiency – the CPU time and time of recording output files on disk. The first one was taken from the standard ECLIPSE output file. The value of the second was taken as the standard Windows file attribute as a difference between the data file time attributes at 1000 and 100 days.

One can see, that the stated in Sect. 4.3 huge CPU advantage of $FTAV$

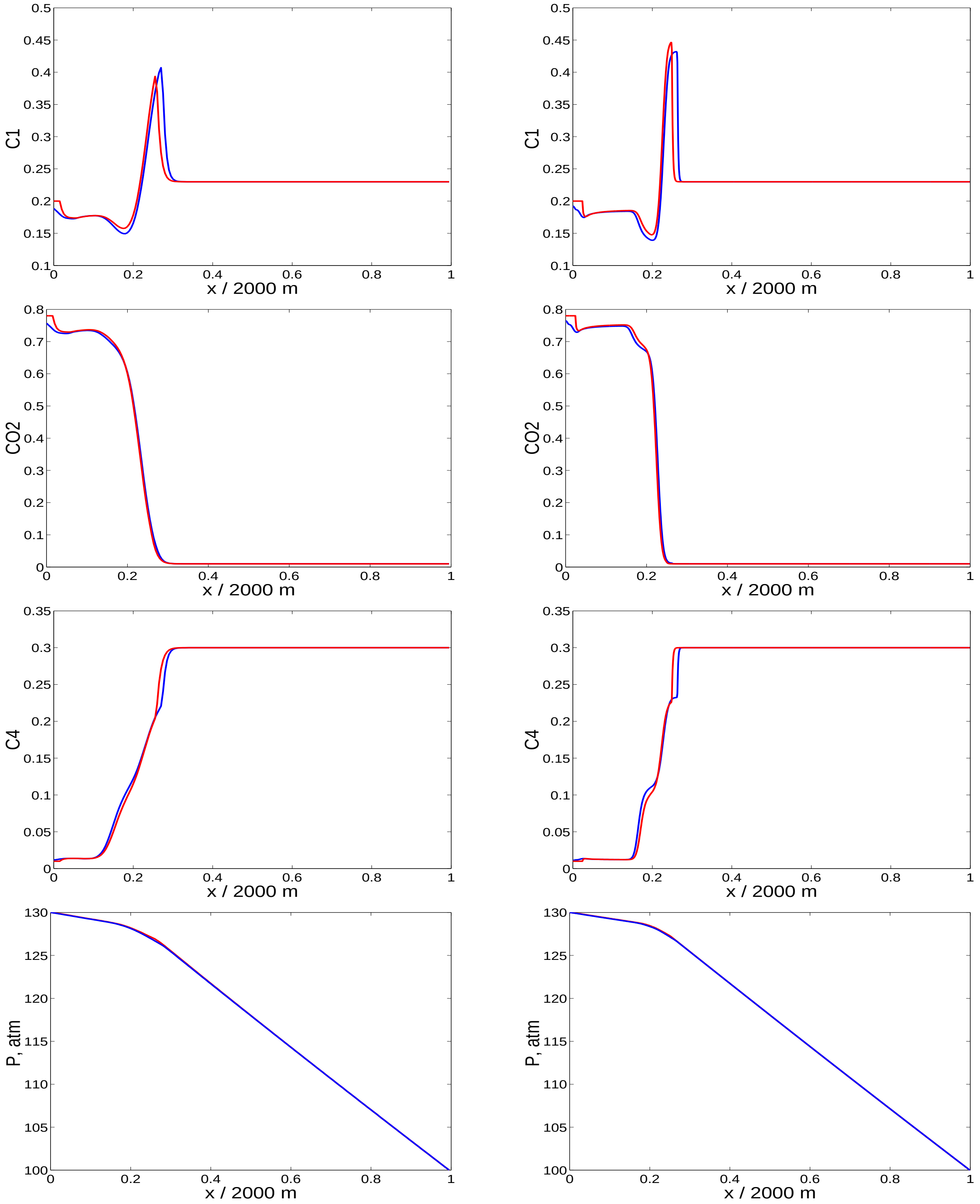

Figure 12: The results of calculations for four-component C1-CO$_2$-C4-C10 mixture are presented at 600 days. The input/output conditions and reservoir parameters are the same as in Fig.1. Blue lines show the solution obtained with modified ECLIPSE package with the *alt*-block, Red lines show the standard ECLIPSE $flashv$ solution. The left column corresponds to the grid with 200 cells, the right - with 1000.

Table 1:

Number of cells	CPU time *alt*-block	CPU time $flashv$	Record disc time *alt*-block	Record disc time $flashv$
200	13.62	14.27	32	32
600	74.61	74.75	112	112
1000	180.57	178.56	237	230

over $flashs$ dissapeared and the efficiences should be considered to be the same. The reason is still unclear but is hidden probably in that we are still far enough from bringing the new inserted subroutines to the highest performance.

6.2 ECLIPSE with RIP

As it is readily seen from Sect. 5, the RIP procedure differs from $FTAV$ procedure only in the way of finding $\boldsymbol{\gamma}$ using specified values of $\boldsymbol{C}$. We recall here for the sake of the reader convenience, that the $FTAV$ technique requires solving the system of $N_c - 1$ equations (28) to find $\boldsymbol{\gamma}$ from the given values of $\boldsymbol{C}$ (subroutine $cresh$), while in the code based on the RIP technique we have to solve only one equation (30) with the fixed k to determine the value of s and then to reconstruct the value of $\boldsymbol{\gamma} = \boldsymbol{\gamma}(s)$ (subroutine crr). Thus, in the case of the four component mixture under consideration, the incorporation of RIP into ECLIPSE package is reduced to the described in the previous Subsection procedure, if the word $cresh$ is replaced by crr and, in addition, the third and fourth components total fractions are calculated in accordance with Eq.(30). Thus, in short the structure of the $altRIP$-block can be described as follows:

1. Polynomial coefficients $P_i^{(k)}$, $P_i^{(m)}$, $P_i^{(d)}$, $P_i^{(b)}$ and $P_i^{(\mu)}$ (see Sect. 4) are read from the hard disk in the beginning of the run, stored in the

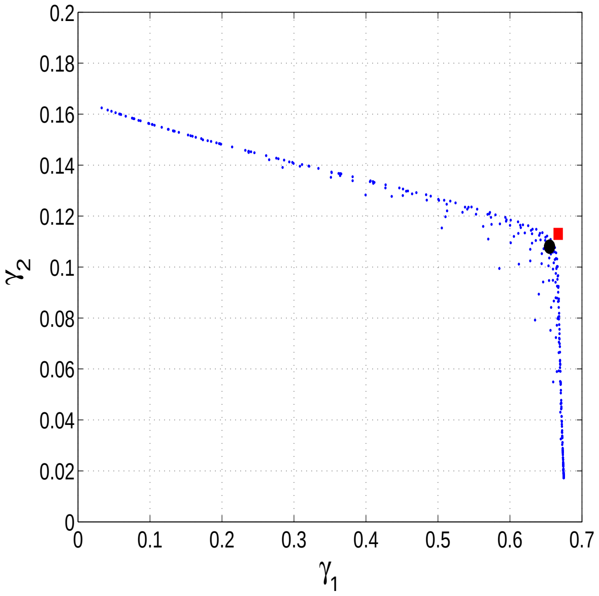

Figure 13: Route in $\boldsymbol{\gamma}$ space for different moments of time for the solutions of 1D oil displacement problems obtained by the ECLIPSE package combined with $FTAV$ technique on the grid 200 cells (blue points). The colores symbols indicate the position of the middle point of three-point quasi-linear approximation of the limiting time independent route.

memory and do not change during calculations.

2. Then total mole fractions SZ are calculated from the given values of molar densities at each iteration in each spatial point.

3. The appropriate approximation of the limiting time-independent route should be chosen. As in Sect. 5 we considered here different three-point quasi-linear approximations for the given route which differ one from another by the choice of the middle point position in $\boldsymbol{\gamma}$ space.

4. At each iteration at each time step loop through cells then starts. During the loop the following procedures are performed:

   a) function *crr* defines the value of s, and, then $\gamma_1(s)$ and $\gamma_2(s)$ using the known values of SZ;

   b) function *cthrmd* determines then component liquid and vapour mole fractions SX and SY

c) then the liquid molar fraction is determined by the given values of SZ, SX and SY. Then SX and SY are updated in single phase areas.

d) the third and fourth components total fractions are evaluated in accordance with equation (30).

5. After all, the Eclipse storage arrays are filled in by the *alt*-block variables SZ, SX and SY;
6. Finally, *cparm* subroutine is called, which is, in fact, the combinaton of standard Eclipse procedures, and aims to fill the rest of $flashv$ output parameters into the Eclipse storage arrays.

To check whether the RIP technique works being incorporated into ECLIPSE we carried out the same numerical experiment as in Sect. 5.2. Namely, we considered the four-component 1D displacement problem, results for which were presented in Figs. 1 and 8. Keeping the value $I_{max} = 200$ and $C1$ as the leading component, we choose CO_2 as the second component in the pseudo three-component system, and $C4$ as the third component. As the middle point of three-point quasi-linear approximation of the limiting time independent route we choose the middle point which gave the best approximation in our in-house simulations, or those in the close vicinity of it. The results are presented in Fig. 14.

One can see, that the choice of the middle point of the curve approximating the route denoted by the black circle in Fig. 13 provides the results that can be considered to be good enough, although we still face some discrepancy of the solutions in the vicinity of injecting well, and the dicrepancy is stronger when the RIP technique is being inserted into ECLIPSE than into the in-house code.

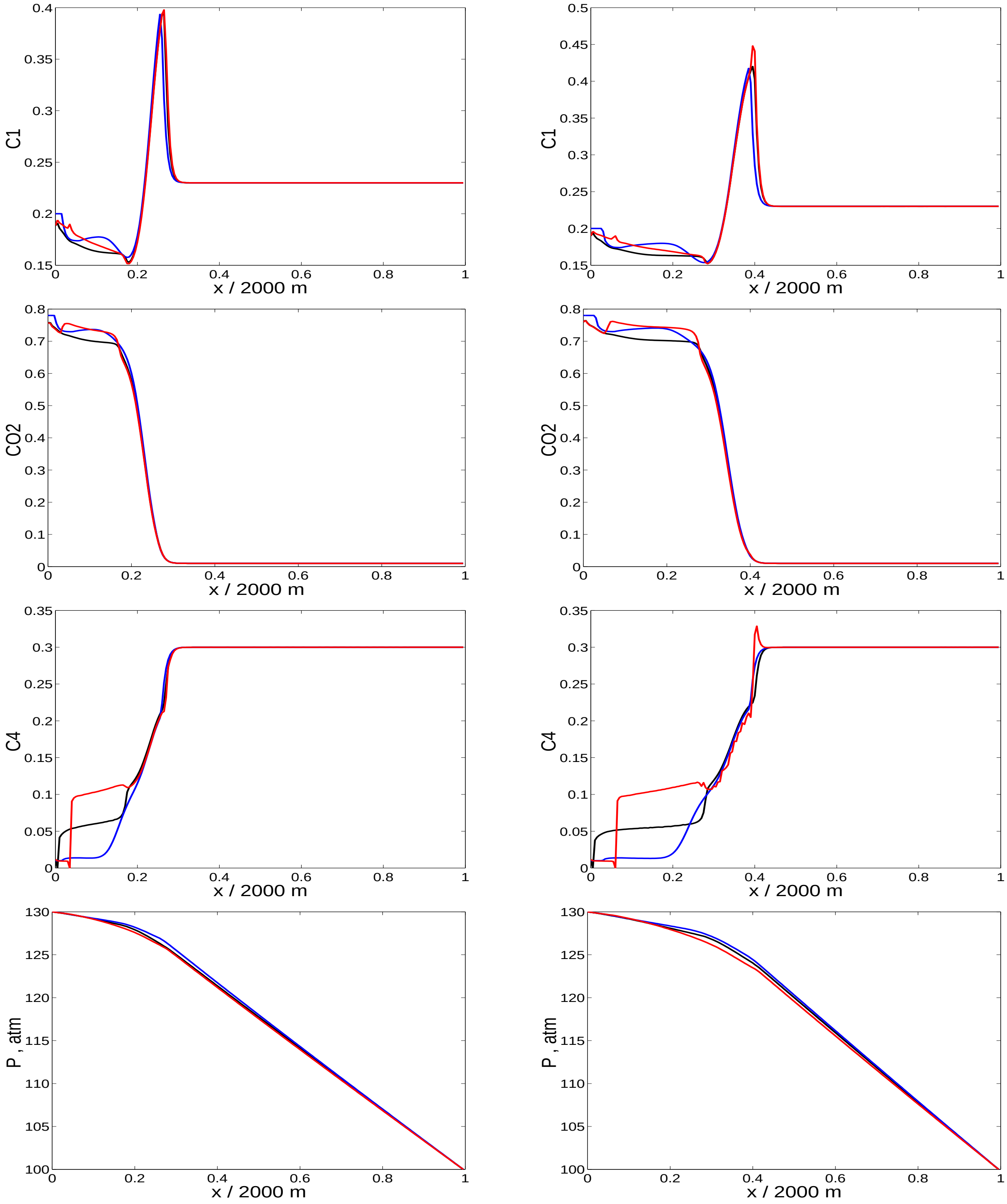

Figure 14: Solutions of the 4-component displacement problem obtained at 600 days (left column) and 900 days (right column) with the help of standard ECLIPSE package (blue) curves, and with ECLIPSE package modified with RIP technique. In the later case the color of the curve corresponds to the color of the symbol in Fig. 13 which indicates the position of the middle point of the three-point quasi-linear approximation of the limiting time-independent route.

7 On approximation of phase equilibrium for multicomponent systems

The alternative description of phase equilibrium described above works efficiently for the systems with up to 10 component. For a larger number of components we face technical problems in the scanning procedure of the composition space, which is still theoretically sound but in practice it is impossible to have enough CPU and RAM facilities to handle the calculation for more than 10 components in reasonable time. The reason is that the number of nodes in the 'composition database' is $T_{max}^{N_c-1}$ (T_{max} is the number of points along each coordinate to be scanned), and it becomes prohibitively large for $N_c = 10 \div 30$.

We examine now several ideas how to extend the developed above technique for the mixtures with number of component exceeding 10. All of them are based on the fact, that in the mixtures with very large number of components one always can distinguish several components whose concentrations are very low initially both in the reservoir and in the injected fluid, and so are expected to remain low during all the displacement evolution.

7.1 Effective Reduction of Scanning Procedure of Phase Diagramm

Let us now return to the schematic scanning procedure of the phase diagram presented in Fig. 3 and suppose that $O2$ there is such a 'minor' component, and its initial concentration does not exceed, say 3 percent both in the reservoir and the injected fluid. That means, that we do not need to run the scanning procedure in $O2$ direction up to the values of $O2$ close to unity, but can stop it when the component concentration becomes comparable with the specified maximum value of initial data with some margin say until it becomes equal to 5 percent.

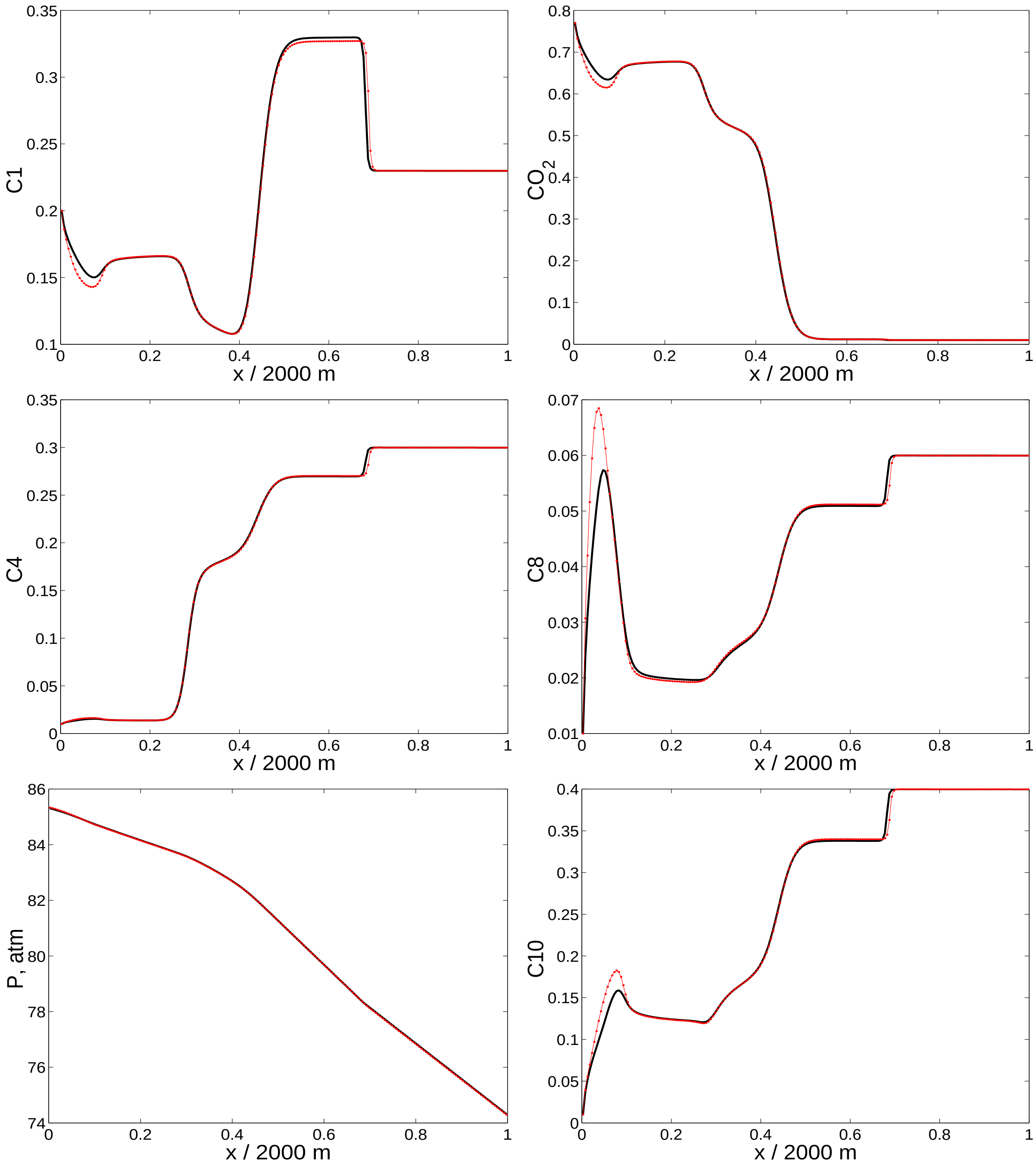

Figure 15: The results of the calculation for the five component C1-CO$_2$-C4-C8-C10 mixture. The inflow/outflow conditions and the reservoir parameters are the same as in Fig. 7. Black lines represent the solution obtained with the γ parametrization help of in-house code with standart $FTAV$ at the moment $t = 1800$ days. Red lines present the solution obtained with the help of the same numerical code, but the beforehand scanning of the phase space was cut in the $C8$ direction at the 10 % levels.

That means that for any slice in the scanning we save a lot of CPU time, and, actually, the procedure for 4-component system presented in Fig. 3 is almost the same as for corresponding 3-component one.

Let us consider again the same 5 component mixture as presented in Fig. 7. Since the $C8$ concentration equals to 6 percent in the injection well and 1 percent in the reservoir, we introduce the cutoff in $C8$ direction at 10-percent level in the scanning procedure. The results of the simulations performed with the help of in-house code with standard $FTAV$ are shown in Fig. 15 by black lines, while red lines correspond to the just described modification. One can note a small discrepancy in the solutions which , however, decreases when the cutoff value increases. Namely, the solutions completely coincide when the value is increased to 15 percent.

7.2 Multicomponent case

To estimate the efficiency of the described above cutting procedure let us assume that the mixture consists of n_c main components and of $N_c - n_c$ additional components, and the maximum concentration of each of this additional component is less than $\delta = 0.1$. Therefore, if we are using, say, $T_{max} = 20$ points along each main coordinate in composition space, we need only 3 points in each 'secondary' composition direction. Then the volume of the compositional space to be scanned is decreased by a factor of $(N_c - n_c)^{10}$. This approach can be effective for as much as 6 main component and up to total number of 10 to 15 components.

However even this limitation of the scanned volume becomes insufficient in the case of very large number of component because it still requires too large amount of calculations.

A way around this obstacle is to once more use the smallness of concentrations of all secondary components, and use linear approximation in these terms for all dependent variables:

$$F(\gamma_1, \ldots, \gamma_{N_c-2}) = F_0(\gamma_1, \ldots, \gamma_{n_c-2}) + \sum_{i=1}^{(N_c-n_c)} F_i(\gamma_1, \ldots, \gamma_{n_c-2})\gamma_{N_c-n_c-2+i}. \tag{32}$$

An important advantage is that due to linearity any composition can be considered as a superposition of $(N_c - n_c)$ compositions of $(n_c + 1)$ component each (say, 30-component mixture state is a superposition of 26 of 5-component systems). Therefore, the number of necessary grid points is $\sim (1/\delta)^{(n_c-1)N_c}$, and becomes quite moderate.

To illustrate the technique, let us return to the structure of approximating polynomials (18) and write it out explicitly in the 5 component case:

$$P[5] = P_1\gamma_1^2+P_2\gamma_2^2+P_3\gamma_3^2+P_4\gamma_1+P_5\gamma_2+P_6\gamma_3+P_7\gamma_1\gamma_3+P_8\gamma_1\gamma_2+P_9\gamma_2\gamma_3+P_{10}.$$

Let us now assume, that γ_3 corresponds to the component with small concentration. If so, we take away this component for a time being, and consider 4 component mixture. For this mixture we obtain the polynomial coefficients exactly in the way described above (Sect. 4.2):

$$P[4] = P_1\gamma_1^2 + P_2\gamma_2^2 + P_3\gamma_1 + P_4\gamma_2 + P_5\gamma_1\gamma_2 + P_6.$$

Then, we fix these coefficients and construct a modified approximating polynomial for the 5 component mixture as follows:

$$P^*[5] = P[4] + (P_6 + P_7\gamma_1 + P_9\gamma_2)\gamma_3 \equiv P[4] + P_{add}.$$

Its structure slightly differs from the structure of the original one since the γ_3^2 term is absent. The coefficients P_6, P_7 and P_9 are evaluated also using the least mean square procedure.

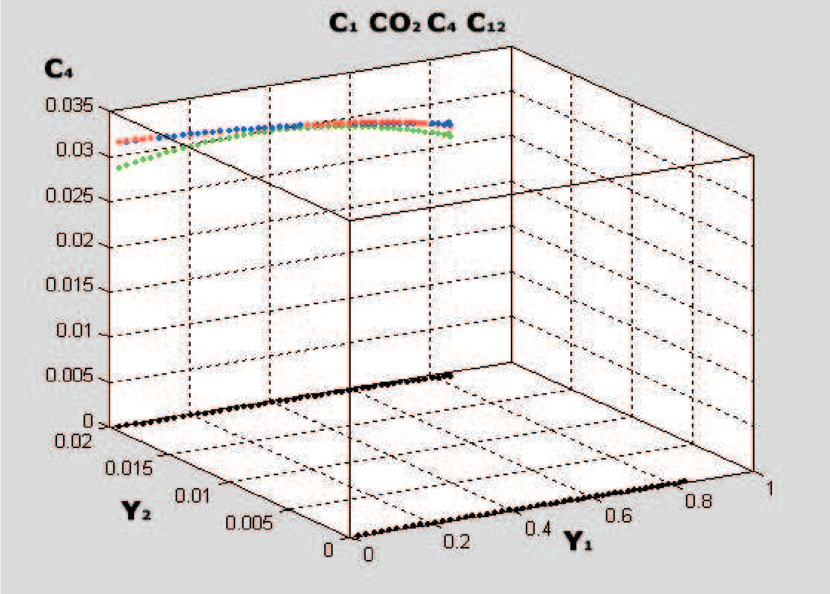

Figure 16: $C1$-CO_2-$C4$-$C12$ mixture with low concentartion of $C4$ is considered. Blue points correspond to the values obtained directly with the help of $flashs$ ECLIPSE procedure, Green points present the result of our standard approximation, and red points correspond to the reconstruction procedure, based on linear approximation of small concentartions instead of quadratic.

Let us suppose that the described procedure of approximation of the 5-component phase space with the help of 4-component model works perfectly, and let us now consider a mixture which consists of the same 4 leading components, and $N = N_c - n_c$ minor components which concentrations are low. Thus, we have (4+N) 5 components systems and the resulting polynomial can be constructed in the similar way as for a single 5-component system.

$$P^*[4+N] = P[4] + \sum_{i=1}^{N} P_{add}.$$

The technique is under the development at the moment. What we can show now is how the reconstruction works in the 4 component case. We considered the following $C1$-CO_2-$C4$-$C12$ mixture where the $C4$ component has low concentration. In Fig. 16, the distributionis of this component in two slices of the $\boldsymbol{\gamma}$ space are presented. Blue points correspond to the values obtained directly with the help of $flashs$ ECLIPSE procedure, Green points present the result of our standard approximation, and red points correspond to the reconstruction procedure, which, as can be seen, works even better than standard one. This is however is well understood since we used linear approximation for the small concentration instead of quadratic.

8 Conclusion

In conclusion, we summarize principal results of the Project.

I. The main achievement of the Project is that a working prototype of an alternative compositional reservoir simulator based on representation of the phase equilibrium in terms of tie-line space parameter has been developed and incorporated into the existing ECLIPSE package.

II. Technically, the crucial new element consists in using *local* change from the standard variables $\{P, \boldsymbol{C}\}$ to the alternative ones $\{P, C_1, \boldsymbol{\gamma}\}$ instead of the *global* change of variables, as was assumed in our previous work [1]-[3].

    This approach made possible to leave intact entire architecture of the code package and all advantages of the best up-to-date algorithms and codes for solution of the reservoir flow problems formulated in the standard variables in the alternative version. Viability of such combined simulator has been tested in a series of numerical experements with the help of a specially developed for this purpose in-house 1D and 2D codes, and with the help of ECLIPSE 300 package as well.

III. Another major achievement of this Project is that a version of the prototype Alternative Simulator using an empirically-established approximate rule of *route invariance* observed in multicomponent flows has been developed and tested. The tests confirm the viability of such simplified version; however they reveal some weak points which apparently can be dealt with in future.

IV. These main advances are supported by research on other topics covered by this Report, such as:

- Development of improved techniques for approximation of phase diagrams in terms of alternative variables.
- Development of fast and robust algorithms of transformation of standard variables into alternative ones and vice versa.
- Development of an interface for interaction of the external 'alternative block' with the main body of the ECLIPSE package.
- Study of the property of route invariance by means of computer experiments.

The main unresolved issue now is whether the alternative approach may lead to significant improvement of computational performance, as it was supposed from the beginning of these studies, or it just provides some advantages in representation and understanding multiphase flows without significant computational gains. This issue can be resolved only by collaborative effort of the main code developers and the research team.

Improvement of efficiency of the alternative simulator requires some more or less straightforward technical work, however it is intimately related to mathematical properties of the governing equtions and computational algorithms including dissipative properties and propagation of discontinuities.

Mentioned above computational and mathematical issues may constitute the backbone of a tentative future project.

References

[1] Entov V.M, Voskov D.V., Turetskaya F.D. Alternative Approach to Compositional Simulations, Report N1, IPM RAS, Moscow, June, 2001

[2] Entov V.M, Voskov D.V., Turetskaya F.D. Alternative Approach to Compositional Simulations, Report N2, IPM RAS, Moscow, Dec. 2001

[3] Entov V.M, Voskov D.V., Turetskaya F.D. Alternative Approach to Compositional Simulations, Final Report, IPM RAS, Moscow, June, 2002

[4] Entov, V.M., in: Proc. of the Conference "Porous Media, Physics, Models, Simulations," Moscow, 19-21 Nov., 1997. A.N.Dmitrievsky, M.B.Panfilov, eds. Singapore, 2000.

[5] Entov, V.M., in: Proc. Intern. Conf. "Modern Approaches to Flows through Porous Media", Moscow, Sept.6-8, 1999, 14-16.

[6] Voskov D.V., Entov V.M., On oil displacement by gas injection: constant partition coefficients case, in: Proc. International Conf. "Modern Approaches to Flows through Porous Media", Moscow, Sept.6-8, 1999, II-32-II-34.

[7] Voskov D.V., and Entov V.M., Izv. RAN, Mekh. Zhidk. Gaza [Fluid Dynamics], 2001, N2, 112-121.

[8] Entov V.M., and Voskov D.V. Effective prediction of multicomponent gas/liquid flows in petroleum reservoirs. Proc. Intern. Conf. on Multiphase Systems, ICMS'2000, Ufa, Russia, June 15-17, 2000, 401-408.

[9] Entov V.M., and Voskov D.V., 2000. Proc of 7th European Conference on the Mathematics of Oil Recovery, Baveno, Italy, 5-8 September 2000. On oil displacement by gas injection.

[10] Entov V.M., Mathematical models oil recovery enhancement by gas injection. "Nauka i tekhnika uglevodorodov",("Hydrocarbon Science and Technology") N6 (13), 2000, 84-90 (in Russian).

[11] Voskov D.V., Two-Phase Multicomponent Flows through Porous Media, PhD Thesis, 2002, Gubkin Russian State Oil and Gas U., Moscow, Russia.

[12] Entov V.M., and Voskov D.V., On approximation of phase equilibria of multicomponent hydrocarbon mixtures and prdiction of oil displacement by gas injection. Submitted: Proc of 8th European Conference on the Mathematics of Oil Recovery, Freiburg, Germany, 4-7 September 2002.

[13] Entov V.M., On theory of multicomponent two-phase flows through porous media, Submitted:*Prikl. Mat. Mekh. [J. Appl. Maths. Mechs.],* 1996.